THE JOURNAL OF PHYSICAL CHEMISTRY A

Article

pubs.acs.org/JPCA

Strength of the Pnicogen Bond in Complexes Involving Group Va Elements N, P, and As

Dani Setiawan, Elfi Kraka,* and Dieter Cremer*

Computational and Theoretical Chemistry Group (CATCO), Department of Chemistry, Southern Methodist University, 3215 Daniel Ave, Dallas, Texas 75275-0314, United States

Supporting Information

ABSTRACT: A set of 36 pnicogen homo- and heterodimers, $R_3E\cdots ER_3$ and $R_3E\cdots E'R'_3$, involving differently substituted group Va elements E = N, P, and As has been investigated at the ωB97X-D/aug-cc-pVTZ level of theory to determine the strength of the pnicogen bond with the help of the local E···E′ stretching force constants k^a. The latter are directly related to the amount of charge transferred from an E donor lone pair orbital to an E′ acceptor σ^* orbital, in the sense of a through-space anomeric effect. This leads to a buildup of electron density in the intermonomer region and a distinct pnicogen bond strength order quantitatively assessed via k^a. However, the complex binding energy ΔE depends only partly on the pnicogen bond strength as H,E-attractions, H-bonding, dipole−dipole, or multipole−multipole attractions also contribute to the stability of pnicogen bonded dimers. A variation from through-space anomeric to second order hyperconjugative, and skewed π,π interactions is observed. Charge transfer into a π^* substituent orbital of the acceptor increases the absolute value of ΔE by electrostatic effects but has a smaller impact on the pnicogen bond strength. A set of 10 dimers obtains its stability from covalent pnicogen bonding whereas all other dimers are stabilized by electrostatic interactions. The latter are quantified by the magnitude of the local intermonomer bending force constants XE···E′. Analysis of the frontier orbitals of monomer and dimer in connection with the investigation of electron difference densities, and atomic charges lead to a simple rationalization of the various facets of pnicogen bonding. The temperature at which a given dimer is observable under experimental conditions is provided.

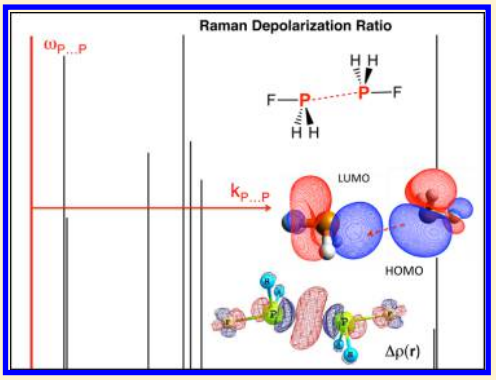

INTRODUCTION

Noncovalent interactions play a key role in chemistry, biology, supramolecular chemistry, and materials science.[1−4] H-bonding with all its facets is the most prominent and well-studied representative.[5−7] However, the number of other stabilizing nonbonbed interactions being recognized is steadily increasing, including dihydrogen bonding,[8] noncovalent halogen-bonding,[9,10] or noncovalent chalcogen-chalcogen interactions.[11−14]

Analyzing the NMR spectra of carborane-phosphino derivatives, Hill and co-workers first discovered the possibility of stabilizing P···P interactions.[15,16] Further evidence for the existence of P···P noncovalent interactions was provided by Drago and co-workers on anion-neutral molecule interactions,[17] Widhalm and Kratky on the synthesis and X-ray structure of binaphthyl-based macrocyclic diphosphanes,[18] and Carré and co-workers on the donor−acceptor (D−A) interactions in three- and four-coordinated phosphorus compounds.[19] Klinkhammer and Pyykkö discussed a closed-shell intermolecular E···E attraction in diphosphine dimers and their chalcogen analogues.[20] In 2003, Wollins and co-workers reported P···P nonbonded interactions in a series of diphospha-functionalized naphthalines.[21] In 2007, Sundberg and co-workers confirmed the P···P noncovalent interactions in 1,2,-dicarba-*close*-dodecaboranes by single crystal X-ray diffractions and DFT calculations[22] supporting the early observations by Hill and co-workers.[15,16] They suggested a hyperconjugative model involving the lone pair electrons of one P atoms and the adjacent σ^*(P−C) orbital. In the same year, Tschirschwitz and co-workers discussed an attractive pnicogen interaction between phosphorus and nitrogen.[23] Tuononen and co-workers synthesized new tetraphoshine ligands with P···P noncovalent interactions,[24] and they showed that the weak interactions between trivalent pnicogen centers are strong enough to lead to supramolecular structures in the solid state.[25] Up to this point, the work on pnicogen bonding was more or less scattered. This changed when the Hey-Hawkins group in collaboration with the Kirchner group demonstrated in their 2011 paper that P···P interactions can be as strong as H-bonds and may be useful molecular linkers.[26] Their investigation was triggered by a study of enantiomerically pure bis(phosphanyl)-carbaborane(12) compounds.[27]

This publication attracted the attention of the chemical community and since then numerous studies on pnicogen bonding have appeared. Experimental investigations were

Special Issue: 25th Austin Symposium on Molecular Structure and Dynamics

Received: August 15, 2014
Revised: October 16, 2014
Published: October 17, 2014

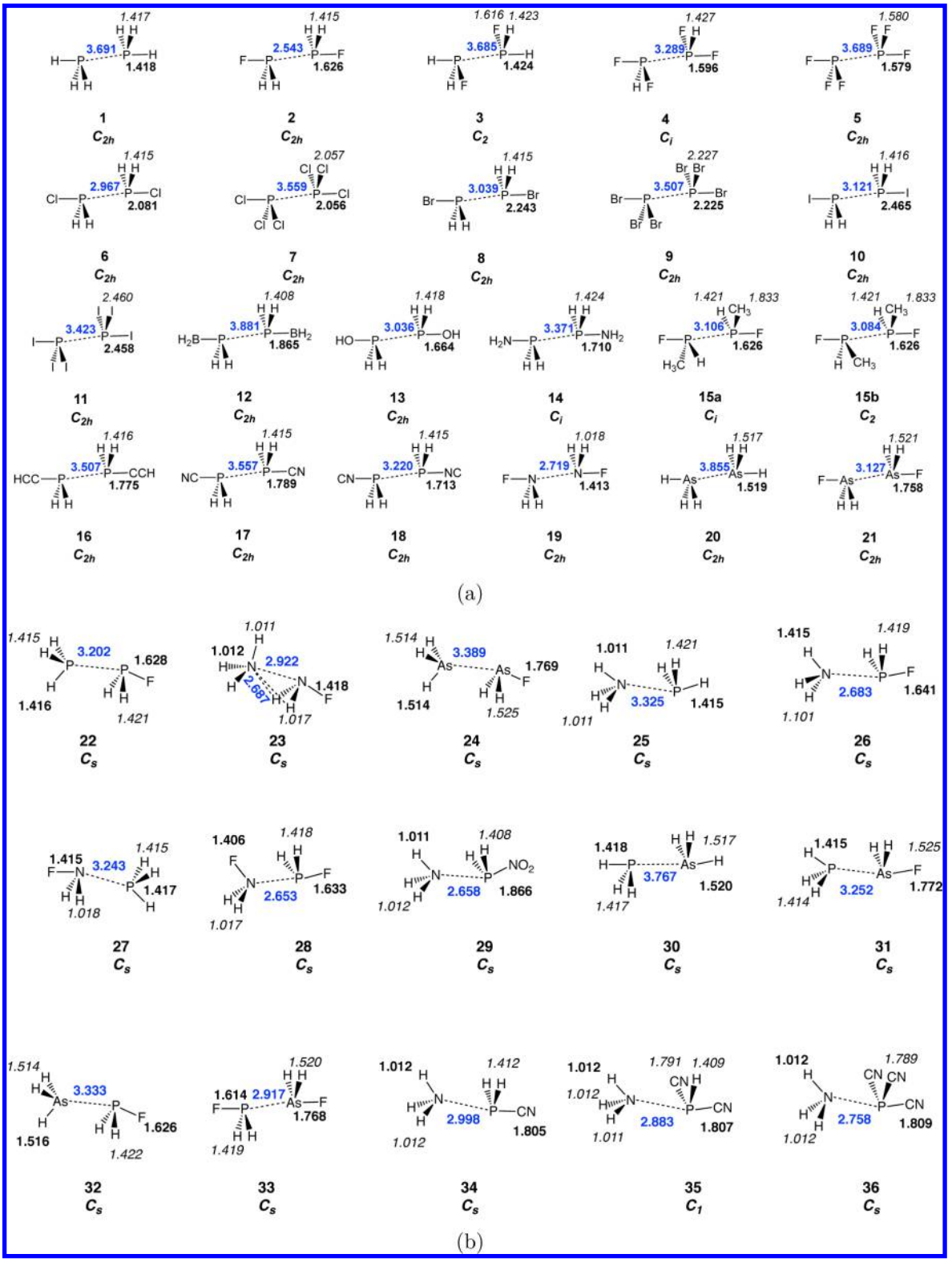

Figure 1. (a) Phosphine homodimers **1**−**21** and (b) phosphine heterodimers **22**−**36** investigated in this work. Numbers in blue correspond to the intermolecular distance in Å, numbers in black (boldface) to pnicogen E−X_{ip} in plane distances, with X being an atom or functional group, and numbers in black (italic) correspond to E−X_{oop} distances. All heterodimers except **33** and **35** adapt a syn form (ωB97XD/aug-cc-pVTZ calculations).

limited to X-ray studies of heavily substituted compounds and ^{13}C or ^{1}H NMR information used for an indirect description of pnicogen bonding. However, numerous quantum chemical studies focused on the investigation of pnicogen bonded complexes targeting predominantly P···P[28−34] and P···N[35−42] interactions, but also extending to E···E′ bonding of the type N···N,[43] P···As,[44] or As···As.[45] Topics include the study of pnicogen−bonding to cation−π complexes,[46] pnicogen-bonded

dx.doi.org/10.1021/jp508270g | J. Phys. Chem. A 2015, 119, 1642−1656

anionic complexes,[47] anion recognition based on pnicogen bonding,[48] pnicogen−hydride interactions in complexes such as $XH_2P\cdots HBeY$,[49] complexes with pnicogen bonds involving sp^2-hybridized phosphorus atoms,[50] intramolecular pnicogen interactions in PHF−$(CH_2)_n$−PHF systems,[51] the interaction of nitryl derivatives and electron donors leading to pnicogen bonds,[52] pnicogen bonding involving nitro compounds and inorganic bromides,[53] single electron pnicogen bonded complexes,[54] and the importance of pnicogen−π complexes for biological systems.[55] Several studies were devoted to a comparison of pnicogen bonding with noncovalent chalcogen, halogen, and H-bonding.[40,56−71] Most of these studies stayed within a well-defined group of pnicogen bonded complexes with similar electronic effects rather than exploring the many facets of pnicogen bonding in more broadly based approach.

Different methodologies have been applied to analyze the nature and the strength of pnicogen-bonded complexes including (i) energy decomposition methods,[72−79] (ii) methods being based on the investigation of the electrostatic potential,[45,80,81] (iii) methods investigating the features of the electron density of the of the pnicogen complexes.[82,83]

In this work, we will pursue a different route by investigating the dynamic aspects of pnicogen bonding as they are revealed by the vibrational modes of a pnicogen-bonded dimer. Vibrational spectroscopy has been amply used to describe H-bonding.[84−91] To the best of our knowledge, no attempts have been made so far to apply vibrational spectroscopy to characterize E···E′ interactions in the same way. However, the interest in the a vibrational characterization of pnicogen bonding may soon be triggered by the availability of terahertz spectroscopy or depolarized Raman scattering, and in this regard the current investigation is timely. With the recent advances in terahertz spectroscopy[92−94] far-infrared absorptions down to 40 cm^{-1} can be recorded and, by this, the measurement of intermolecular pnicogen−pnicogen vibrations is feasible.

We have recently performed a comprehensive analysis of H-bonding based on local vibrational modes.[90] In this work, we will apply the local vibrational mode analysis of Cremer and co-workers[95−98] to a representative test set of 36 pnicogen complexes **1**−**36** (Figure 1), which includes homo dimers and hetero dimers for E = N, P, and As, a variety of different substituents X of E covering, and a range of different E···E′ interactions. Our investigation also requires that dimers **1**−**36** are compared with the corresponding monomers **M1**−**M24** and suitable reference molecules **R1**−**R10**, which are described in the Supporting Information. The main goal of our work is (i) to elucidate the interplay of electronic and electrostatic factors determining the dimer stability and (ii) to provide a quantitative measure of the pnicogen bond strength based on vibrational modes, derived either from experiment or from calculations.

COMPUTATIONAL METHODS

In this work, equilibrium geometries and normal vibrational modes were calculated using the ωB97X-D density functional,[99,100] which was chosen because it provides a reliable description of noncovalent interactions in cases where dispersion and other long-range van der Waals interactions play an important role.[62,101−103] For the same reason, Dunning's aug-cc-pVTZ basis sets[104−106] were used. For Br and I, the Stuttgart effective core potentials (ECPs)[107] were employed in connection with the cc-pVTZ-PP basis sets.[108,109] In the case of Br, it was verified (by comparison with the corresponding cc-pVTZ-PP results) that the use of an ECP does not affect calculated vibrational frequencies significantly.

The DFT calculations were carried out using an ultrafine grid and tight convergence criteria in the geometry optimizations to guarantee a reliable calculation of vibrational frequencies. To verify the utility of the ωB97X-D functional, dimers **1**, **2**, **6**, **8**, and **10** were reoptimized at the CCSD(T) level of theory[110] employing the same basis sets. Similar results were obtained, however, with the general observation that pnicogen bonding is somewhat weaker.

Calculated binding energies ΔE of the dimers were corrected for basis set superposition errors (BSSE) employing the counterpoise method of Boys and Bernardi.[111] Free binding energies $\Delta G(T)$ were calculated at T = 298, 100, and 5 K to determine the temperature T(obs) at which ΔG becomes negative, thus providing a chance of observing a given dimer and characterizing it by experimental means.

The charge-transfer analysis was carried out on the basis of calculated NBO (natural bond order) charges.[112,113] A topological analysis of the electron density distribution $\rho(\mathbf{r})$ was performed.[114] The nature of the pnicogen bond was determined by the energy density $H(\mathbf{r})$ calculated at the bond critical point $\mathbf{r}_b$ and the application of the Cremer−Kraka criteria for covalent bonding: (i) A zero-flux surface and bond critical point r_b have to exist between the atoms in question (necessary condition). (ii) The local energy density at $H(\mathbf{r}_b)$ must be negative and thereby stabilizing (sufficient condition for covalent bonding). A positive $H(\mathbf{r}_b)$ indicates a dominance of electrostatic interactions.[115,117] Hence, the Cremer−Kraka criteria can reveal whether pnicogen bonding is covalent, electrostatic, or a mixture of both (values close to zero).

Electron difference density distributions $\Delta\rho(\mathbf{r}) = \rho$(dimer AB) − [$\rho$(monomer A) + ρ(monomer B)] were calculated at the ωB97X-D/aug-cc-pVTZ level of theory using for the monomers A and B the geometries they adopt in the dimer. Orbital energies for the determination of the HOMO−LUMO gaps of donor (D) and acceptor (A) monomers have been calculated at the Hartree−Fock (HF) level using the 6-31G(d,p) basis set.[118] For iodine the 6-311G(d,p) basis set was used.[119]

The local vibrational modes were derived according to Konkoli and Cremer.[95,96] All vibrational mode and electron density calculations were carried out with the program package COLOGNE2014,[120] whereas for the CCSD(T) calculations CFOUR[121,122] and MOLPRO,[123] and for the DFT calculations Gaussian09[124] was used.

DESCRIPTION OF PNICOGEN BONDING WITH THE HELP OF VIBRATIONAL SPECTROSCOPY - A NEW AVENUE

Normal vibrational modes probe the electronic structure and the bonds of a molecule or a molecular complex. Therefore, the stretching force constants should provide a direct measure of the strength of the corresponding bond and the bending force constants about bond−bond interactions based on hybridization, electrostatic, and polarization effects.[95−98,125,126] In this connection, one has to consider that normal vibrational modes are generally delocalized because of mode coupling. Specific bond information can only be extracted from the calculated or measured vibrational frequencies if the coupling between the vibrational modes is suppressed and local vibrational modes are obtained, as has been shown by Cremer and co-work-

Table 1. Calculated Properties of Dimers 1−36 and Reference Molecules R1−R10[a]

	molecule (sym)	R	ΔE	ΔG (298)	ΔG (100)	ΔG (5)	T(obs)	ω^a	k^a	n	ρ_b	H_b	H_b/ρ_b
1	$(PH_3)_2$ (C_{2h})	3.691	−1.15	5.21	1.38	−0.43	28	65.0	0.039	0.032	0.043	0.005	0.123
2	$(PH_2F)_2$ (C_{2h})	2.543	−5.87	6.70	−0.72	−3.94	116	156.2	0.223	0.151	0.384	−0.110	−0.285
3	$(PH_2F)_2$ (C_2)	3.685	−0.93	7.22	2.30	−0.25	13	60.0	0.033	0.027	0.047	0.005	0.106
4	$(PHF_2)_2$ (C_i)	3.289	−1.47	6.48	1.77	−0.78	33	78.6	0.056	0.044	0.098	0.000	0.000
5	$(PF_3)_2$ (C_{2h})	3.689	−0.60	6.66	2.05	−0.34	17	58.6	0.031	0.029	0.048	0.005	0.096
6	$(PH_2Cl)_2$ (C_{2h})	2.967	−3.12	7.18	0.93	−2.14	72	83.3	0.063	0.049	0.171	−0.017	−0.100
7	$(PCl_3)_2$ (C_{2h})	3.559	−1.85	5.21	1.04	−1.43	63	75.6	0.052	0.041	0.060	0.005	0.077
8	$(PH_2Br)_2$ (C_{2h})	3.039	−2.90	7.00	0.99	−2.05	70	71.1	0.046	0.037	0.150	−0.011	−0.074
9	$(PBr_3)_2$ (C_{2h})	3.507	−2.93	4.79	0.02	−2.77	108	85.1	0.066	0.051	0.065	0.005	0.073
10	$(PH_2I)_2$ (C_{2h})	3.121	−2.36	7.24	1.42	−1.60	57	83.1	0.065	0.050	0.130	−0.006	−0.047
11	$(PI_3)_2$ (C_{2h})	3.423	−4.61	4.29	−1.18	−4.28	148	83.2	0.065	0.050	0.079	0.004	0.052
12	$(PH_2BH_2)_2$ (C_{2h})	3.881	−1.05	6.16	1.84	−0.60	27	54.4	0.027	0.023	0.030	0.005	0.161
13	$(PH_2OH)_2$ (C_{2h})	3.036	−3.27	6.94	0.71	−2.27	77	80.0	0.058	0.045	0.148	−0.011	−0.075
14	$(PH_2NH_2)_2$ (C_i)	3.371	−2.00	5.83	1.08	−1.44	60	82.9	0.063	0.049	0.076	0.003	0.042
15a	$(PHFCH_3)_2$ (C_i)	3.106	−4.07	6.02	−0.10	−3.19	105	89.9	0.074	0.056	0.140	−0.009	−0.062
15b	$(PHFCH_3)_2$ (C_2)	3.084	−4.20	6.41	−0.07	−3.32	104	89.4	0.073	0.056	0.140	−0.009	−0.062
16	$(PH_2CCH)_2$ (C_{2h})	3.507	−1.66	5.82	1.32	−1.15	50	62.5	0.036	0.030	0.061	0.004	0.074
17	$(PH_2CN)_2$ (C_{2h})	3.557	−0.96	8.01	2.29	−0.51	22	64.5	0.038	0.031	0.058	0.005	0.080
18	$(PH_2NC)_2$ (C_{2h})	3.220	−1.98	8.71	1.90	−1.28	43	85.1	0.066	0.051	0.104	−0.001	−0.010
19	$(NH_2F)_2$ (C_{2h})	2.719	−3.60	5.34	0.01	−2.55	100	178.0	0.131	0.086	0.088	0.017	0.190
20	$(AsH_3)_2$ (C_{2h})	3.855	−1.26	3.77	0.91	−0.69	46	32.1	0.023	0.018	0.039	0.003	0.087
21	$(AsH_2F)_2$ (C_{2h})	3.127	−2.94	6.78	0.92	−2.03	71	63.7	0.090	0.066	0.145	−0.010	−0.071
22	$H_3P\cdots PH_2F$ (C_s)	3.202	−3.44	4.75	−0.16	−2.45	105	71.9	0.047	0.038	0.108	−0.001	−0.010
23	$H_3N\cdots NH_2F$ (C_s)	2.922	−4.09	2.92	−1.09	−2.98	153	196.8	0.160	0.099	0.068	0.016	0.229
24	$H_3As\cdots AsH_2F$ (C_s)	3.389	−3.66	4.05	−0.48	−2.76	123	55.5	0.068	0.051	0.090	0.000	0.003
25	$H_3N\cdots PH_3$ (C_s)	3.325	−1.64	4.27	0.94	−0.56	40	86.8	0.043	0.015	0.051	0.007	0.143
26	$H_3N\cdots PH_2F$ (C_s)	2.683	−6.49	2.80	−2.44	−4.65	190	172.8	0.170	0.055	0.166	−0.005	−0.031
27	$FH_2N\cdots PH_3$ (C_s)	3.243	−2.04	4.58	0.65	−1.29	68	57.6	0.019	0.007	0.056	0.009	0.160
28	FH_2NPH_2F (C_s)	2.653	−5.36	4.14	−1.42	−3.96	149	144.0	0.118	0.039	0.175	−0.007	−0.042
29	$H_3N\cdots PH_2NO_2$ (C_s)	2.658	−7.56	2.10	−3.31	−5.68	221	159.3	0.144	0.047	0.180	−0.009	−0.047
30	$H_3P\cdots AsH_3$ (C_s)	3.767	−1.21	3.83	0.92	−0.62	43	49.3	0.031	0.024	0.042	0.004	0.103
31	$H_3P\cdots AsH_2F$ (C_s)	3.252	−4.20	3.90	−0.95	−3.26	139	86.9	0.098	0.070	0.107	0.000	−0.002
32	$H_3As\cdots PH_2F$ (C_s)	3.333	−3.03	5.23	0.35	−2.00	86	77.6	0.078	0.057	0.092	0.000	0.000
33	$FH_2P\cdots AsH_2F$ (C_s)	2.917	−4.21	6.22	−0.03	−2.99	100	89.3	0.103	0.074	0.201	−0.026	−0.127
34	$H_3N\cdots PH_2(CN)$ (C_s)	2.998	−4.73	3.45	−1.24	−3.40	151	136.5	0.106	0.035	0.094	0.007	0.073
35	$H_3N\cdots PH_2(CN)_2$ (C_1)	2.883	−7.59	1.77	−3.58	−5.95	232	148.8	0.126	0.041	0.121	0.004	0.036
36	$H_3N\cdots PH_2(CN)_3$ (C_s)	2.758	−10.11	−0.65	−6.00	−8.30	324	168.1	0.161	0.052	0.161	−0.002	−0.015
R1	P_2H_4 (C_2)	2.219						647.6	1.845	1.000	0.783	−0.403	−0.515
R2	P_2H_2 (C_{2h})	2.013						662.6	4.006	2.000	1.044	−0.738	−0.707
R3	N_2H_4 (C_2)	1.424						1025.5	4.338	1.000	2.075	−1.667	−0.803
R4	N_2H_2 (C_{2h})	1.231						1681.5	11.663	2.000	3.394	−4.859	−1.431
R5	As_2H_4 (C_2)	2.452						261.8	1.513	1.000	0.590	−0.237	−0.402
R6	As_2H_2 (C_{2h})	2.226						375.4	3.111	2.000	0.798	−0.439	−0.551
R7	H_2P-NH_2 (C_1)	1.708						786.6	3.516	1.000	1.115	−0.979	−0.878
R8	HP=NH (C_s)	1.572						1129.5	7.249	2.000	1.418	−1.256	−0.886
R9	H_2P-AsH_2 (C_1)	2.341						358.7	1.661	1.000	0.671	−0.303	−0.452
R10	HP=AsH (C_s)	2.122						519.1	3.480	2.000	0.906	−0.559	−0.617

[a]Pnicogen bond distances R (Å), dimer binding energies ΔE (kcal/mol), dimer free binding energies ΔG (kcal/mol) at 298, 100 and 5 K respectively, estimated temperature T(obs) at which the dimers are stable, local E···E′ stretching frequencies ω^a (cm^{-1}), local E···E′ stretching force constants k^a (mdyn/Å), relative bond strength order n, electron densities ρ_b ($e/Å^3$) at the bond critical point $\mathbf{r}_b$, energy densities H_b (hartree/$Å^3$), and ratio H_b/ρ_b (hartree/e), calculated at the ωB97XD/aug-cc-pVTZ level of theory.

ers.[95,96,125,127] Experimentally, this has been accomplished via the *isolated stretching frequencies* of McKean[128] or the overtone spectra, which lead to local mode frequencies in special cases.[129] A general computational solution has been found by Konkoli and Cremer,[95] who showed that mode−mode coupling includes electronic and kinematic (mass) coupling. Their way of determining local vibrational modes is closely related to Wilson's solution of the vibrational problem.[130] Wilson showed that by solving the Euler−Lagrange equations the basic equation of vibrational spectroscopy is obtained:[130]

$$\mathbf{F}^q\mathbf{D} = \mathbf{G}^{-1}\mathbf{D}\Lambda \quad (1)$$

where $\mathbf{F}^q$ is the calculated force constant matrix expressed in internal coordinates q_n, $\mathbf{D}$ collects the vibrational eigenvectors $\mathbf{d}_\mu$ in the form of column vectors (μ = 1, ..., N_{vib} with $N_{vib} = 3N - L$; N is the number of atoms; L is the number of translations

dx.doi.org/10.1021/jp508270g | J. Phys. Chem. A 2015, 119, 1642−1656

Table 2. Local Intermonomer Bending Force Constants k^a (mdyn/rad^2) and the Corresponding Local Mode Frequencies ω^a (cm^{-1})

♯	Dimer (Sym)	k^a_{512}	ω^a_{512}	k^a_{621}	ω^a_{621}	k^a_{312}	ω^a_{312}	k^a_{421}	ω^a_{421}
1	$(PH_3)_2$ (C_{2h})	0.027	153.7			0.025	148.3	0.025	148.3
2	$(PH_2F)_2$ (C_{2h})	0.286	503.5			0.226	147.9	0.226	147.9
3	$(PH_2F)_2$ (C_2)	0.025	148.6			0.025	147.8	0.025	147.8
		0.047	53.4						
4	$(PHF_2)_2$ (C_i)	0.022	38.6			0.008	26.8	0.008	26.8
		0.287	197.0						
5	$(PF_3)_2$ (C_{2h})	0.007	21.5			0.005	21.5	0.005	21.5
6	$(PH_2Cl)_2$ (C_{2h})	0.096	290.6			0.073	62.5	0.073	62.5
7	$(PCl_3)_2$ (C_{2h})	0.038	35.8			0.037	41.7	0.037	41.7
8	$(PH_2Br)_2$ (C_{2h})	0.083	270.5			0.067	53.6	0.067	53.6
9	$(PBr_3)_2$ (C_{2h})	0.061	38.6			0.044	40.5	0.044	40.5
10	$(PH_2I)_2$ (C_{2h})	0.066	240.9			0.053	43.9	0.053	43.9
11	$(PI_3)_2$ (C_{2h})	0.086	42.4			0.050	40.2	0.050	40.2
12	$(PH_2BH_2)_2$ (C_{2h})	0.025	146.9			0.022	43.0	0.022	43.0
13	$(PH_2OH)_2$ (C_{2h})	0.105	302.6			0.085	88.3	0.085	88.3
14	$(PH_2NH_2)_2$ (C_i)	0.029	159.0			0.034	54.7	0.034	54.7
		0.029	160.5						
15a	$(PHFCH_3)_2$ (C_i)	0.086	274.5			0.173	122.3	0.173	122.3
		0.199	119.8						
15b	$(PHFCH_3)_2$ (C_2)	0.110	309.3			0.184	126.2	0.184	126.2
		0.196	119.7						
16	$(PH_2CCH)_2$ (C_{2h})	0.020	131.9			0.013	33.4	0.013	33.4
17	$(PH_2CN)_2$ (C_{2h})	0.012	101.0			0.022	43.5	0.022	43.5
18	$(PH_2NC)_2$ (C_{2h})	0.007	78.1			0.003	17.1	0.003	17.1
19	$(NH_2F)_2$ (C_{2h})	0.022	196.5			0.027	73.0	0.027	73.0
20	$(AsH_3)_2$ (C_{2h})	0.010	86.0			0.008	78.0	0.008	78.0
21	$(AsH_2F)_2$ (C_{2h})	0.031	152.5			0.018	29.4	0.018	29.4
22	$H_3P\cdots PH_2F$ (C_s)	0.138	345.9	0.032	169.7	0.113	98.6	0.026	151.6
23	$H_3N\cdots NH_2F$ (C_s)	0.021	190.9	0.017	175.7	0.531	316.5	0.058	321.0
24	$H_3As\cdots AsH_2F$ (C_s)	0.155	337.5	0.026	140.3	0.136	80.0	0.026	140.0
25	$H_3N\cdots PH_3$ (C_s)	0.006	101.4	0.070	248.3	0.012	150.3	0.063	238.4
26	$H_3N\cdots PH_2F$ (C_s)	0.043	280.2	0.351	556.5	0.062	337.6	0.325	182.3
27	$FH_2N\cdots PH_3$ (C_s)	0.018	176.2	0.010	92.2	0.009	39.5	0.006	75.1
28	$FH_2N\cdots PH_2F$ (C_s)	0.020	188.4	0.208	428.4	0.048	91.0	0.189	140.2
29	$H_3N\cdots PH_2NO_2$ (C_s)	0.071	359.5	0.320	535.3	0.077	374.6	0.284	165.9
30	$H_3P\cdots AsH_3$ (C_s)	0.014	100.5	0.011	96.5	0.013	100.2	0.011	98.7
31	$H_3P\cdots AsH_2F$ (C_s)	0.172	356.6	0.034	173.3	0.144	85.3	0.029	161.5
32	$H_3As\cdots PH_2F$ (C_s)	0.028	145.2	0.149	358.0	0.027	141.8	0.127	101.5
33	$FH_2P\cdots AsH_2F$ (C_s)	0.118	296.8	0.081	266.7	0.079	65.2	0.056	69.5
34	$H_3N\cdots PH_2(CN)$ (C_s)	0.026	217.4	0.164	381.2	0.036	257.7	0.143	119.0
35	$H_3N\cdots PH_2(CN)_2$ (C_1)	0.062	337.2	0.208	430.2	0.061	331.5	0.214	147.5
		0.076	370.9	0.373	169.1				
36	$H_3N\cdots PH_2(CN)_3$ (C_s)	0.100	426.6	0.456	190.0	0.107	440.5	0.327	185.0

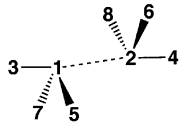

[a]Local oop bending force constants k^a_{512}, k^a_{621}, and ip bending force constants k^a_{312}, k^a_{421}. Force constant k^a_{712} is given for dimers with C_2 or C_i symmetry (**4**, **14**, **15a**, **15b**, **35**), k^a_{821} for dimers with C_1 symmetry (**35**).

and rotations), **G** is the Wilson matrix for the kinetic energy,[130] and **Λ** is a diagonal matrix containing the vibrational eigenvalues $\lambda_\mu = 4\pi^2c^2\omega_\mu{}^2$ (ω_μ: vibrational frequency of mode $\mathbf{d}_\mu$). Solution of the Wilson equation implies the diagonalization of matrix $\mathbf{F}^q$ to give the diagonal matrix **K**. In this way, the electronic coupling between the local modes is eliminated. The local mode approach of Konkoli and Cremer suppresses also the kinematic coupling by starting from the mass-decoupled Euler−Lagrange equations.[95] Zou and Cremer have recently demonstrated that in this way the mass-decoupled equivalent of the Wilson equation[97,98] is obtained, which by diagonalization directly leads to the local vibrational modes $\boldsymbol{a}_n$ being associate with internal coordinates q_n:[95,97,98,131]

$$\mathbf{a}_n = \frac{\mathbf{K}^{-1}\mathbf{d}_n^\dagger}{\mathbf{d}_n\mathbf{K}^{-1}\mathbf{d}_n^\dagger} \tag{2}$$

where $\mathbf{d}_n$ is a row vector of matrix **D**. The local mode force constant k^a_n is given by eq 3

$$k^a_n = \mathbf{a}_n^\dagger\mathbf{K}\mathbf{a}_n \tag{3}$$

and the local mode frequency ω^a_n can be obtained from

$$(\omega^a_n)^2 = \frac{G_{nn}k^a_n}{4\pi^2c^2} \tag{4}$$

where element G_{nn} of matrix **G** defines the local mode mass.[95] Each local mode is associated with a specific structural unit of a molecule, which in turn can be described by a single internal coordinate: one-bond diatomic units characterized by a bond length, two-bond triatomic units characterized by a bond angle, etc. In this way, the local stretching, bending, or torsional force constants describe the strength of the chemical bond, the stiffness of bending (caused by hybridization, polarization, and

dx.doi.org/10.1021/jp508270g | J. Phys. Chem. A 2015, 119, 1642−1656

other electrostatic effects), or the height of the rotational barrier.

The force constant k^a of an AB stretching mode (A and B being bonded) is a reliable measure for the AB bond strength.[132−135] This does not hold for the local frequency ω^a, which depends also on the masses of atoms A and B thus disguising the electronic origin of the bond strength. When a large set of k^a values is compared, the use of a relative bond strength order (BSO) n is convenient.[132−135] The relative BSO n(EE′) is obtained by utilizing the extended Badger rule,[126,135,136] according to which n is related to the local stretching force constant k^a by a power relationship, which is fully determined by two reference values and the requirement that for a zero-force constant n becomes zero. In this work, we used $H_2E{-}E'H_2$ and HE═E′H molecules **R1**−**R10** as reference with n = 1 and 2, respectively, leading to the following parameters a and b of the power relationship: a(PP) = 0.578 and b(PP) = 0.894; a(NP) = 0.300 and b(NP) = 0.958; a(AsAs) = 0.672 and b(AsAs) = 0.962; a(PAs) = 0.622 and b(PAs) = 0.937; a(NN) = 0.358 and b(NN) = 0.701.

THE MECHANISM OF PNICOGEN BONDING

In Table 1, the properties of dimers **1**−**36** and reference molecules **R1**−**R10** (Figure 1) calculated at the ωB97XD/aug-cc-pVTZ level of theory are listed. These comprise the E···E′ distance R, the binding energy ΔE and the corresponding free energy value, $\Delta G(T)$ (T = 298, 100, and 5 K), the estimate of T(obs) for which the dimer in question becomes observable, the local E···E′ stretching frequency ω^a and force constant k^a, the relative BSO n, the electron density ρ_b at the E···E′ bond critical point $\mathbf{r}_b$, the corresponding energy density H_b, and the ratio H_b/ρ_b. Table 2 contains the local ip and oop (intermonomer) bending force constants XE···E′ for complexes **1**−**36**. Utilizing these values, we will in the following describe pnicogen bonding where we will first focus on a comparison of **1** with **2** because the latter dimer is a prototypical example for E···E′ bonding. NBO charges of the homodimers **1**−**21**, reference molecules **R1**−**R10**, and monomers **M1**−**M24** as well as the NBO charges and the charge-transfer values for the heterodimers **22**−**36** are given in the Supporting Information.

Pnicogen Bonding between Two PH_2F Monomers. In Figure 2, two-electron (2e) stabilizing and four-electron (4e) destabilizing interactions between two monomers **M2** are schematically shown where Figure 2b gives on the left perspective drawings of the lone pair lp(P) and σ*(PF) orbital of D- and A-monomer. If two NH_3 (**37a** in Figure 3) or PH_3 molecules (**1a**) collide head-on as shown in Figure 3, the 4e destabilizing interaction (lp repulsion) dominates. Accordingly, the electron difference density distribution $\Delta\rho(\mathbf{r})$ reveals a strong depletion of electron density in the intermonomer region (blue color) for both **37a** and **1a**. This changes for **1** when it adopts its equilibrium geometry: A slight electron density increase (red, Figure 3) in the intermonomer region reveals the influence of a charge transfer from one monomer to the other as a consequence of the 2e-stabilization interactions indicated in Figure 2a. If the NH_3 dimer is arranged in a similar way (**37** in Figure 3 represents a saddle point of second order), there is only depletion of electron density in the intermonomer region. This has to do with the fact that the σ*(NH) orbital contrary to the σ*(PH) orbital has a larger coefficient at H (because of the electronegativity difference between N and H and the orthonormality between σ and σ* MOs). Hence, the orbital overlap of the frontier orbitals required for the charge

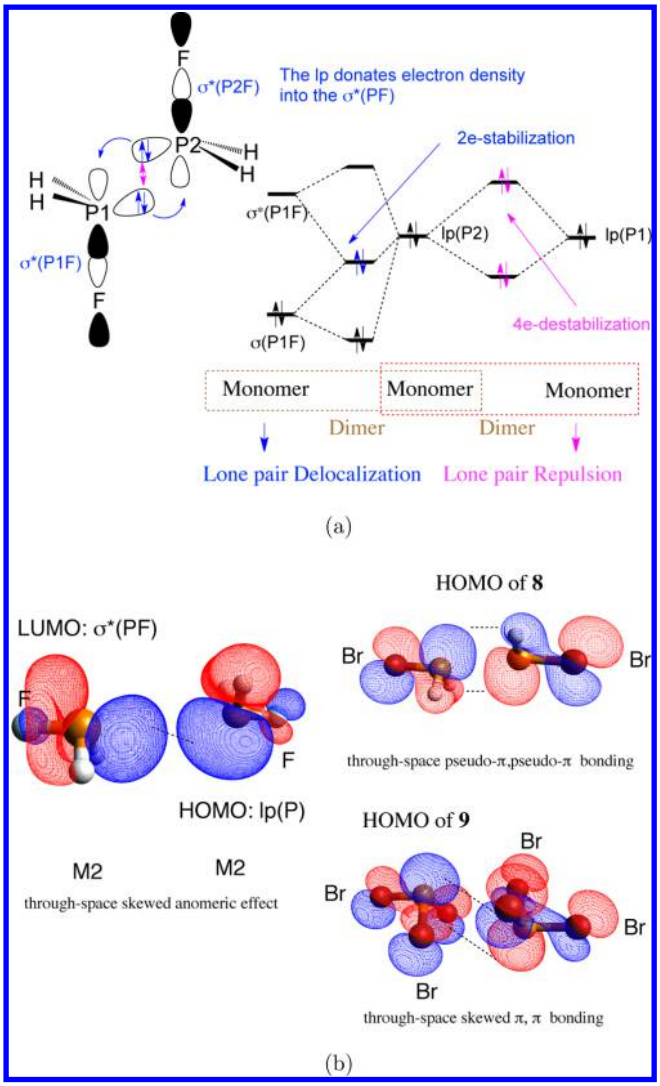

Figure 2. (a) Schematic representation of an orbital interaction diagram for pnicogen bonding between two PH_2F monomers. On the right, destabilizing 4e-interactions (lone pair(lp) repulsion between lp(P1) and lp(P2), purple color) is shown. Each of the lp orbitals can undergo a 2e-stabilizing interaction with a σ* orbital (blue color), which leads to a charge transfer into the latter and some covalent character of pnicogen bonding. (b) Perspective drawings of the LUMO (σ*(PF)) and HOMO (lp(P)) involved in pnicogen bonding between monomers **M2** (PH_2F, left) as well as the HOMO of dimers **8** and **9** are shown. The dominating interactions are given by dashed lines and the nature of bonding is indicated.

transfer and the 2e-stabilization is too small. Lp repulsion continues to dominate.

An increase of the 2e-stabilizing interactions (Figure 2a) is accomplished if the PX electronegativity difference increases, thus lowering the energy of the σ*(PX) MO, increasing its coefficient at P, and thereby its overlap with the lp-orbital of the approaching second monomer. This is shown for the LUMO of PH_2F (Figure 2b), which bulges out into the intermonomer space. Consequently, any charge-transfer (2e-stabilizing) interaction leads to an increase of electron density in the intermonomer region, which is clearly visible from the difference density $\Delta\rho(\mathbf{r})$ of **2** in Figure 3. At the same time the electron density of the PF bond is depleted, causing a lengthening (weakening) of this bond by 0.007 Å. Because both monomers can function as D and A, there is a mutual

dx.doi.org/10.1021/jp508270g | J. Phys. Chem. A 2015, 119, 1642−1656

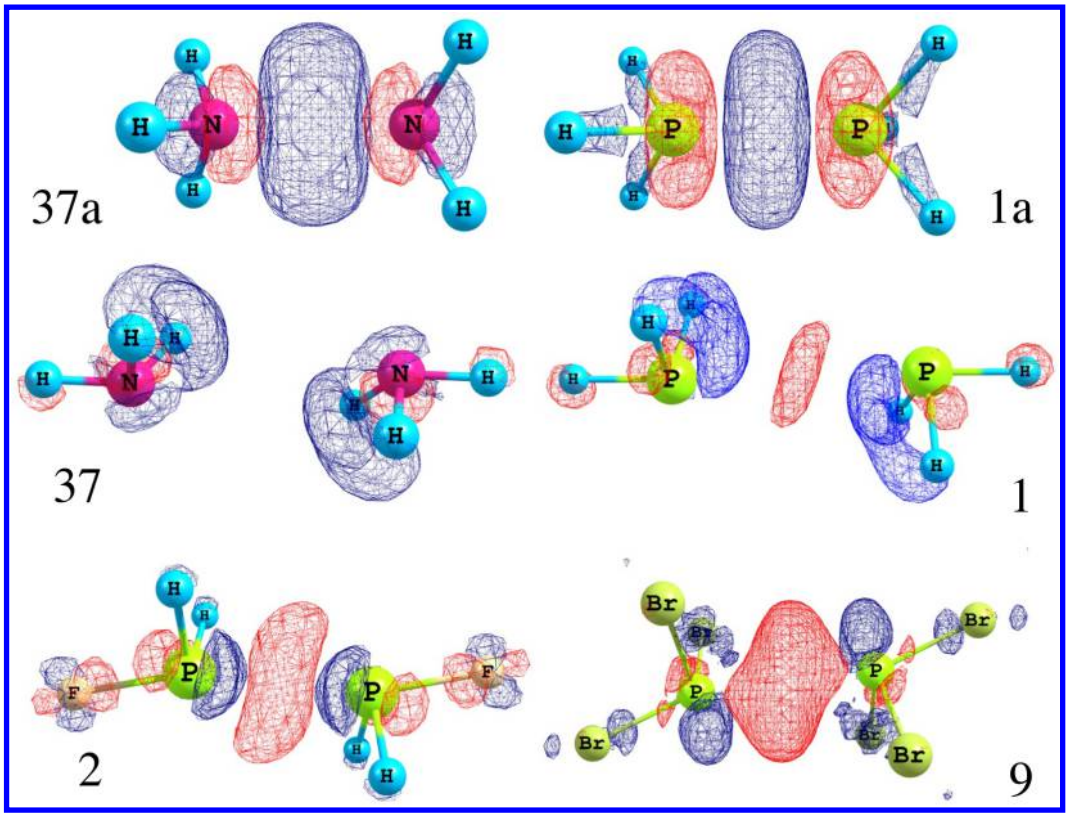

Figure 3. Perspective drawings of the electron difference density distribution $\Delta\rho(\mathbf{r}) = \rho(\text{dimer AB}) - [\rho(\text{monomer A}) + \rho(\text{monomer B})]$ where the geometries of the monomers were adjusted to the dimer geometries. Red contour lines indicate an increase of $\Delta\rho(\mathbf{r})$, blue contour lines a decrease.

enhancement of the D and A ability (charge transfer leads to a lowering of the σ^* MO of the D monomer and raising of the lp-orbital of the A monomer). The P···P distance decreases from 3.7 Å in **1** to 2.543 Å. The binding energy of (**2**) is −5.87 kcal/mol, comparable to that of the H-bond in the water dimer (−5.0 kcal/mol[91]). The resulting E···E bond is the strongest of all P···P dimers investigated in this work. It is characterized by a large k^a value of 0.223 mdyn/Å, ρ_b of 0.384 e/Å^3, and H_b/ρ_b of −0.285 hartree/e (Table 1).

As the orbital diagram in Figure 2a reveals, the 2e-stabilization effect between two **M2** resembles an (intramolecular) anomeric effect[137,138] and might be considered as *through-space anomeric delocalization*. Closer inspection of the frontier orbitals of homodimers such as **8** or **9** (see the dimer HOMOs in Figure 2b) reveals that the HOMO has through-space pseudo-π,pseudo-π-character in line with second-order hyperconjugation,[139] which leads to some slight π-character of pnicogen bonding. The basic features of through-space lp-electron delocalization have been invoked by a number of authors[37,39,41,56,58,68] as the dominant driving force for pnicogen bonding.

However, the examples in Figure 3 reveal that, apart from the geometrical requirements of any through-space anomeric delocalization, which must be as such that head-on lp-repulsion is largely avoided, there is also a distortion of the monomer charge distribution, which speaks of additional polarization effects apart from the multipole interactions between the monomers. Therefore, it is understandable that other authors have emphasized the role of the electrostatic interactions between the monomers.[29,50,80,81,140] Clearly, charge-transfer and electrostatic interactions both play a role and must not be considered exclusively as is also true for any dispersion interactions.[25]

Generally, the complex binding energy ΔE (in the following often discussed by its absolute value $|\Delta E|$) is taken as an indicator for the strength of pnicogen bonding. However, this is a serious simplification as ΔE is a cumulative measure of the strength of the E···E′ bond and all additional interactions between the substituents of E or E′. The local E···E′ stretching force constant gives for the first time the possibility of separately describing pnicogen bonding and detailing additional electronic effects, which together determine the dimer stability. The current analysis will be carried out in a way that will address the dimensionality and complexity of pnicogen bonding. Therefore, we will (i) differentiate between homo- and heterodimers, (ii) consider a variation in the E, E′ bonding partners (E = N, P, As), (iii) investigate a variety of E-substituents, and (iv) discuss a syn and an anti approach of the monomers.

P···P Pnicogen Homodimers. In Figure 4, the relationship between relative BSO values n and the local P···P stretching force constant k^a is shown. BSO values stretch from 0.02 (PH_2BH_2 dimer (**12**)) to 0.151 (**2**). The majority of PP-homodimers have BSO values in the range 0.027−0.056. Hence, dimer **2** is exceptional as it has the strongest pnicogen bond, which is confirmed by the electron density ρ_b at the bond critical point and a strongly negative H_b value (Table 1 and Figure 5). According to the Cremer−Kraka criteria, **2** possesses a bond with significant covalent character.

The discussion given in the previous subsection indicates that the prerequisites for significant covalent character are multiple: (a) The orbital energy gap $\Delta\varepsilon$ between HOMO(D) and LUMO(A) must be small, which is fulfilled if E(D) is not too

dx.doi.org/10.1021/jp508270g | J. Phys. Chem. A 2015, 119, 1642−1656

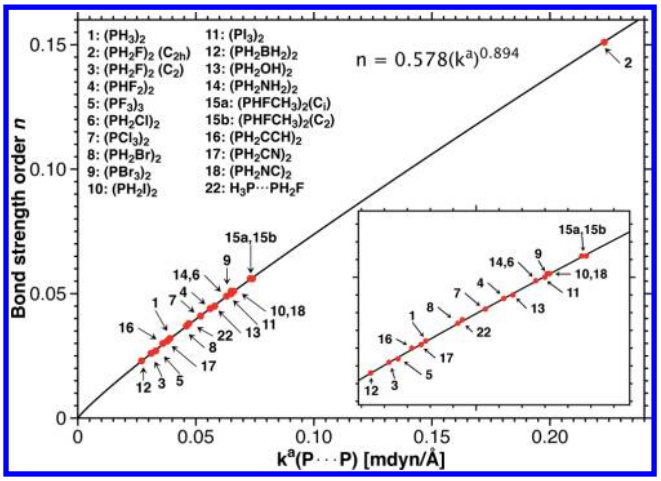

Figure 4. Relationship between bond strength order n and local P···P stretching force constant k^a.

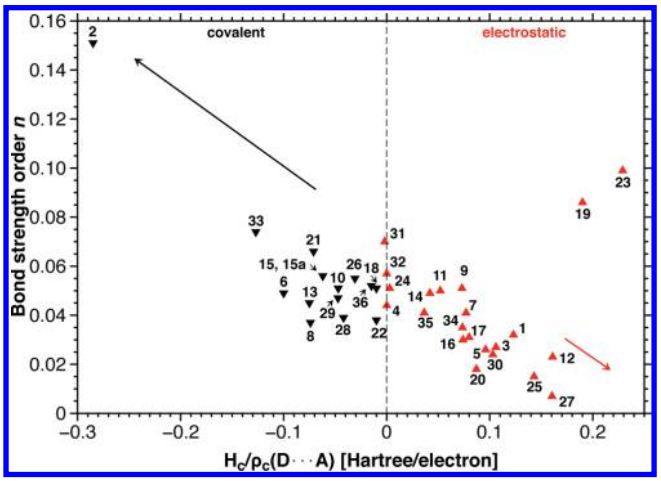

Figure 5. Relationship between the bond strength order n and the ρ_b-normalized energy density $H_c = H_b$ at the bond critical point $\mathbf{r}_b$(E···E′). Covalent interactions are given by black triangles, and electrostatic interactions, by red triangles.

electronegative (the lp orbital energy is relatively high) and X in E′X is significantly more electronegative than E′(A). The latter prerequisite guarantees that both the σ(E′X) (lowering 4e-destabilization with the lp(E) orbital) and σ^* (E′X) (closing the gap with the lp(E) orbital) are lower in energy. (b) The overlap between the frontier orbitals must be large in the intermonomer region to support the charge transfer. (c) Charge transfer must increase the electron density in the intermonomer region. Otherwise, it leads to stabilization of the dimer without leading to a relatively strong pnicogen bond.

The parent dimer **1** has a HOMO−LUMO $\Delta\varepsilon$ of 0.5509 hartree ($\Delta\varepsilon$(**2**) = 0.5139 hartree), thus leading to a small anomeric delocalization. This is confirmed by ΔE(**1**) = −1.1 kcal/mol, a P···P distance of 3.691 Å being longer than the P···P van der Waals distance of 3.6 Å,[141] and the small P···P stretching force constant k^a of 0.039 mdyn/Å (Table 1).

The necessity of a low-lying ip σ^* orbital is demonstrated by moving the F atoms in **2** into one of the oop positions as realized in dimer **3**. The strong stabilization of **2** vanishes and a situation similar to that of **1** is obtained. The binding energy of −0.9 kcal/mol for **3** is (absolutely seen) smaller than that of **1** (−1.15 kcal/mol). The BSO value is 0.027 (the second lowest of all 36 dimers investigated) according to a k^a value of 0.033 mdyne/Å, both reflecting a weak P···P interaction.

Increasing the fluorination of the phosphine dimer changes the nature of the P atoms. They become more positively charged (1269 me in **4**, 1704 me in **5** compared to 680 me in **2**). The covalent radius of P is reduced and the lone pair energies decrease (**M2**, −0.3898 hartree; **M3**(PHF_2), −0.4071 hartree; **M4**(PF_3), −0.4590 hartree). Because the energies of the σ^*(PF) orbitals also somewhat increase, the frontier orbital gap significantly increases (**M2**, 0.5139 hartree; **M3**, 0.5375 hartree; **M4**, 0.6024 hartree), thus reducing through-space anomeric delocalization. In addition, the overlap between lp(P) and σ^* orbitals is reduced because of the contraction of the former orbital so that a much smaller delocalization effect for **4** and **5** results, thus leading to stabilization energies of −1.47 and −0.60 kcal/mol (Table 1). The P···P stretching force constants are small and the energy densities positive, thus indicating that only electrostatic attractions keep the monomers in **4** and **5** together. This confirms Scheiner's finding that, in contrast to H-bonding, bis- or tris-halogen substitution does not necessarily produce any additional complex stabilization.[142]

In dimers **6**, **8**, and **10**, the F atoms of **2** are replaced by X = Cl, Br, and I, respectively. With increasing atomic number of X, its electronegativity decreases, which causes an increase of the energy of σ(PX) and σ^*(PX) and, thereby, of the HOMO−LUMO gap. Through-space interactions are reduced, the P···P distances become longer, and the ip PX distances and the P charges resemble more those of the monomers. The binding energies decrease (absolutely seen) to −2.36 kcal/mol (**10**).

In this connection, one has to note that the lp orbitals of halogenated phosphine or arsine dimers have no longer the typical sp^3-hybridized form of NH_3 but adopt pπ-character with an antibonding EX contribution as shown in Figure 2b. With increasing atomic number of E and X, the charge transfer takes place more and more in the off-line E···E region (i.e., between lp and oop CX bonds), as is nicely revealed by the difference density of **2** (Figure 3). The HOMO of the dimer (see, e.g., **8** in Figure 2b) adopts pseudo-π,pseudo-π character with decreased antibonding character for the ip PX bond (leading to reduced PX lengthening).

$(PX_3)_2$ dimers with X = F, Cl, Br, and I (**5**, **7**, **9**, and **11**) do not follow the same pattern as the $(PH_2X)_2$ dimers. The ΔE values decrease from −0.60 kcal/mol (**5**) to −4.61 kcal/mol (**11**), which is in line with the decreasing P···P distance R (Table 1). However, the k^a(P···P) values of **5**, **7**, **9** first increase as expected (0.031, 0.052, 0.66 mdyn/Å) but the k^a(**11**) = 0.65 mdyn/Å does not continue this increase.

The lp orbital of EX_3 complies with the C_{3v} symmetry of the molecule; i.e., it is basically a pπ(E) orbital oriented along the C_3 axis mixing in an antibonding fashion with the pπ(X) orbitals. Accordingly, the monomer LUMO has σ^*(PX) character but at P local 4s character, which is distorted in the dimer formation. Due to the mutual polarization of the monomers, a new type of interactions results (HOMO of **9**, Figure 2b), which can be described as a through-space skewed π, π interaction. The HOMO of the dimer adopts some ip PX bonding character, and therefore, these bonds are now shorter (rather than longer, Figure 1) in the dimer when compared with those of the corresponding monomers.

The X_{ip}E···E angles decrease from close to 180° to values below 160° (157° for **11**), the values of R become smaller (3.423 Å for **11** compared to 3.689 Å for **5**), and the difference density confirms the picture of a *skewed π-bond* resulting from

dx.doi.org/10.1021/jp508270g | J. Phys. Chem. A 2015, 119, 1642−1656

$\sigma-\pi$-mixing (Figures 2b and 3). Mutual polarization between the electron densities of P and the oop X atoms enhance this effect (see blue depletion regions at the oop Br atoms and P of **9** (Figure 3). Skewed π, π bonding increases with the polarizability of X (or the extension of its pπ AOs into space). The oop XP···P bending force constants increase from just 0.007 (X = F), 0.038 (Cl), 0.061 (Br) to 0.086 (mdyn Å)/rad^2 (I), and the corresponding ip values increase from 0.005 to 0.050 (mdyn Å)/rad^2 (Table 2).

The local intermonomer bending force constants correlate with the calculated ΔE values (Figure 6b) when comparing

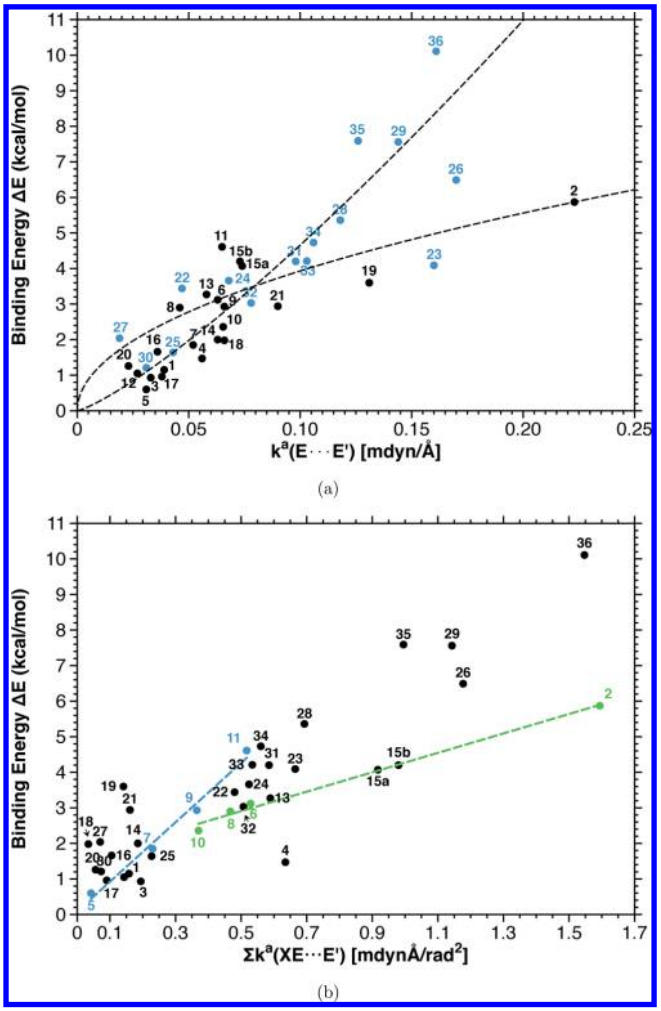

Figure 6. (a) Relationship between binding energy $|\Delta E|$ and the local pnicogen stretching force constant k^a(E···E′). Blue dots indicate heterodimers, for which D and A can be distinguished. (b) Relationship between binding energy $|\Delta E|$ and the sum of all intermonomer bending force constants $\sum k^a$(XE···E′). For related dimers such as **5**, **7**, **9**, **11** (blue dashed line), or **2**, **6**, **8**, **10** (green dashed line), linear relationships between ΔE and $\sum k^a$(XE···E′) are obtained.

$|\Delta E|$ with the sum of k^a(XE···E′) values for a group of related dimers such as **5**, **7**, **9**, **11** (blue dashed line in Figure 6b), or **2**, **6**, **8**, **10** (green dashed line), for which linear relationships of different ascent are obtained.

The analysis of the monomer orbitals confirms the charge-transfer picture even in the case of $(PX_3)_2$ dimers where previous investigations tended to prefer an explanation on the basis of electrostatic interactions. Clearly, any π-type overlap reduces the density accumulation along the E,E′ connection line and leads to a positive energy density at the (3,−1) critical point. Hence, the pnicogen interactions in **5**, **7**, **9**, and **11** are electrostatic whereas in **2**, **6**, **8**, and **10** they are all covalent. This is not a contradiction to the charge-transfer description used above because electrostatic interactions can also be rationalized in terms of orbital interactions.

Our results are in line with observations made by Tuononen and co-workers who suggested that the increase in the $|\Delta E|$ is in line with the increase of the softness of the halide X.[25] The increase in the softness leads to an increase in charge polarization in the PX_3 monomers. It has been argued that electrostatic and polarization interactions are typical of E···E bonding and lead to its angular characteristics.[29,31,39,50,57] Schreiner and co-workers suggested that pnicogen bonding is highly directional showing a large anisotropy with respect to the ip bond angle distortion, which is even larger than that of H-bonding.[42,56,69−71] Adhikari and Scheiner[69] discussed the sensitivity to these distortions qualitatively via a harmonic potential obtained from distorting the fully optimized complex geometry in 1−10° increments and fitting the data points with a parabola. This is a numerical approach, which we replace here by an analytical, more accurate one provided by the local bending force constants (Table 2).

It has been suggested that electronegative substituents X help to strengthen the E···E interactions by increasing the charge transfer from the lp to the σ^* orbital, provided the substituents are chosen in a way that the HOMO−LUMO gap remains small.[37,39,41,56,58,68] One can qualitatively monitor the increased charge transfer through the shortening of the E···E distance R and the lengthening of the P−X bond. The local P···P stretching force constant k^a introduced in this work provides a quantitative measure.

In the series X = BH_2 (**12**), NH_2 (**14**), OH (**13**), and F (**2**), $|\Delta E|$ increases and R decreases (Table 1). The local P···P stretching force constant k^a for X = BH_2 is much smaller (0.027 mdyn/Å) than that for **2** (0.223 mdyn/Å). However, the k^a values for X = NH_2 (0.063) and X = OH (0.058 mdyn/Å) are reversed. This is due to the fact that the charge transfer into the σ^*(PO) orbital is disturbed by the σ lp orbital at the O atom (P···POH angle: 180°). However, the local bending constant k^a(HP···P) of **13** is more than 3 times larger than that of **14** (0.105 vs 0.029 (mdyn Å)/rad^2, Table 2), reflecting that oop polarization makes up for the reduced charge transfer. This example confirms that the local mode forces constants unravel even small details of E···E bonding and the interactions between the monomers. It also confirms that there cannot be a general and quantitative correlation between $|\Delta E|$ and R (Supporting Information).

According to ωB97x-D, there is a weakly stabilized AsH_3 dimer (**20**) but not a stable NH_3 dimer directly connected by a N···N bond. In contrast to **2** and **20**, the H atoms in NH_3 are strongly positively charged (−8 me PH_3; −39 me AsH_3; 352 me $H_3N{\cdots}PH_3$ (**25**);Supporting Information). This leads to the well-known N···H bonding rather than stabilizing N···N interactions as discussed above. Scheiner found a direct N···N interaction when one of the H atoms in one of the NH_3 monomers is replaced by F (**23**). However, as indicated in Figure 1, there also also contributions from N···H bonding between the H atoms of the NH_2F and the N of the NH_3 monomer. This is reflected by the fact that ΔE is with −4.09 kcal/mol relatively large in magnitude as is the local N···N stretching force constant of 0.160 mdyn/Å. However, this is not

dx.doi.org/10.1021/jp508270g | J. Phys. Chem. A 2015, 119, 1642−1656

a result of charge transfer (see below) but additional H-bonding, which is in line with the fact that the ip HN···N bending constant is with 0.531 (mdyn Å)/rad^2 the largest calculated in this work, thus reflecting the stiffness of the geometry of **23**.

Pnicogen Heterodimers. The dominating charge transfer in the heterodimers **22**−**36** can be determined and rationalized following the line of investigation applied in the previous subsection. In the way, one direction of charge transfer dominates, the antiarrangements of EX(ip) and E′X(ip) bonds is no longer a prerequisite of the mutual charge transfer and the ip bonds can rearrange to minimize lp-repulsion and maximize attractive interactions between the lp(E′) and the positively charged oop H atoms in the case of E = N (**25**, **29**, **34**−**36**) or the negatively charged oop H atoms with the positively charged E′ atom (P or As in the case of **22**, **24**, **30**, **31**, and **32**) as was verified in this work by studying frontier orbitals and NBO charges (given in the Supporting Information). In all these cases, a syn arrangement of the EX bonds results with XE···E angles being in the range 111−148° when NH_3 or XNH_2 D-monomers are involved and 130−142° for D-monomers with E = P or As.

Because of these additional stabilizing effects, the stability of the heterodimers can be significantly larger than that of the homodimers as is shown in Table 1. The most stable heterodimers investigated in this work, **26**, **29**, **35**, and **36**, have ΔE values of −6.49, −7.56, −7.59, and −10.11 kcal/mol, respectively. The magnitude of the charge transfer from the D-monomer to the A-monomer is related to the energy gap between HOMO(D) and LUMO(A) (Figure 2a). However, when the two monomers approach each other, polarization can change this gap as discussed above and as recently shown by a block-localized wave function (BLW) analysis of Mo and co-workers.[35] As mentioned, the local mode stretching constant k^a reflects that part of the charge transfer that leads to an electron density increase in the intermonomer region. Because of its local nature, it does not account for the electrostatic attraction between substituents not leading to any change in E···E′ bonding strength. In this way, the local mode analysis helps to separate charge-transfer and substituent-linked electrostatic effects.

In Figure 6a, the relationship between $|\Delta E|$ and k^a is shown and in Figure 7, the magnitude of the charge transfer from D to A is compared with the very same k^a values. The black dots for the homodimers in Figure 6 cluster around a power relationship (using **2** and **6** as reference points) for the cases with covalent E···E bonding with clear deviations for those systems with a different interaction mechanism depending on mutual polarization as discussed above. The heterodimers seem to follow a linear (or exponential) relationship; however, scattering from this line is much stronger. Again, it holds that ΔE is the result of all electronic effects stabilizing the dimers whereas k^a reflects just the strength of pnicogen bonding.

Using the MO model of Figure 2, it is easy to predict the prevailing charge-transfer direction from D to A. A will be always the monomer that contains an ip EX bond with a suitable σ^*(EX) orbital with the following properties: (i) low energy; (ii) a large lobe contribution at E resulting from a large electronegativity difference between E and X and/or a diffuse (polarizable) ns/np contribution with high n. In this regard, PH_2F is a better A than FH_2N in **28**, AsH_2F better than FH_2P in **33**, PH_3 better than H_3N in **25**, AsH_3 better than H_3P in **30**, or PH_3 better than FH_2N in **27**. A new situation results if the

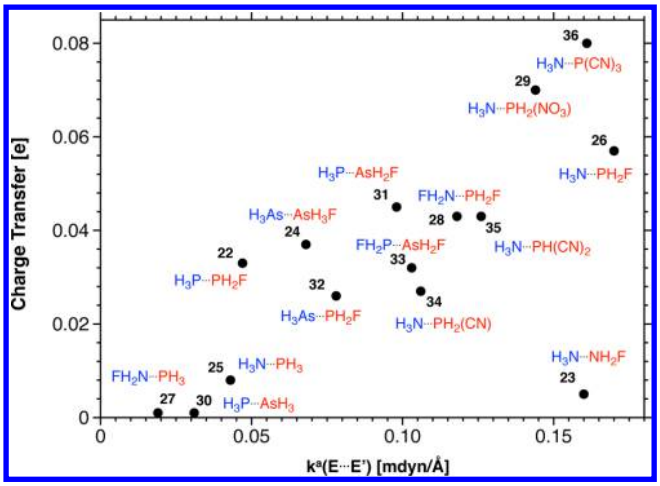

Figure 7. Relationship between charge transfer from D to A and the local pnicogen stretching force constant k^a for the heterodimers **22**−**36**. The D-monomer is indicated by the blue, and the A-monomer, by the red.

electronegative ip substituent X has also a low lying π^* orbital such as CN or NO_2, which leads to an increase in the A-capability (see below).

In heterodimers **23**, **25**, **27**, and **30**, charge transfer is small because of relatively large HOMO(D)−LUMO(A) gaps. This is not directly obvious in the case of **27**, but it becomes clear when realizing that PH_3 is the better A, which leaves FH_2N the role of the D, thus causing a larger orbital gap. In all these cases, both k^a and $|\Delta E|$ values are relatively small with the exception of **23**, which is stabilized by additional H-bonding (see above). Molecule **23** is a striking example for the fact that a large $|\Delta E|$ value does not necessarily imply a strong pnicogen bond.

Heterodimers **22**, **24**, **31**, and **26** follow the trends discussed (charge transfer increasing from 33 to 57 me, k^a from 0.047 to 0.170 mdyn/Å, $|\Delta E|$ from 3.44 to 6.49 kcal/mol, Table 1) and underline that the A-ability is complemented by the polarizing power of the D, which increases the D−A charge transfer. In this regard, H_3P is stronger in polarizing AsH_2F in **31** than H_3As is in polarizing AsH_2F in **24** where the strongest complex in this series is **26**, obtaining its strength from the fine-tuned combination of the polarizing power of H_3N and the A-ability of PH_2F. In a similar way, the increase of charge transfer, k^a value, and $|\Delta E|$ in the series **32**, **33**, and **35** can be explained. All explanations are based on the inspection of the frontier orbitals, NBO charges, and difference densities of monomers and dimers. This analysis confirms that also the polarization effects can be anticipated from the frontier orbitals. We note that in the case of **26**, the dimer stability is increased by dipole,dipole attractions, which are always possible if the D is equal to NH_3 and the A-monomer contains an EX bond with X being more electronegative than E.

Heterodimers **29**, **34**, **35**, and **36** represent a different pnicogen bonding mechanism. In **29**, the charge transfer is mediated by the σ^*(PN) orbital but the actual A is the π^* of the NO_2 group. This is reflected by the lengthening of the PN and NO bonds by 0.023 and 0.03 Å, and the increase of the N and O charges by 13 and 27 me, respectively, relative to the isolated A-monomer. A charge transfer to the NO_2 group does not significantly increase the density in the intermonomer region. Accordingly, k^a is smaller than one would expect from a ΔE = −7.56 kcal/mol and corresponds more to an exponential

dx.doi.org/10.1021/jp508270g | J. Phys. Chem. A 2015, 119, 1642−1656

increase of $|\Delta E|$ with k^a as is indicated by the dashed line (passing through **29**) in Figure 6a. The local intermonomer bending constants of PH_2NO_2 in **29** are large, thus indicating that electrostatic effects between the substituents increase $|\Delta E|$ and decrease R to 2.658 Å, which is the smallest R value of all molecules investigated in this work (Table 1).

A similar analysis of charge transfer, k^a, and ΔE values explains the unusual stability of the cyano substituted complexes **35** and **36**. Heterodimer **36**, with −10.11 kcal/mol, is the most stable complex investigated in this work. The intermonomer bending force constants for **36** (0.327 mdyn/Å) are the largest of all complexes investigated and describe a situation similar to that of **9** and **10** discussed above.

COMPARISON WITH OTHER PNICOGEN BOND MODELS AND CONCLUSIONS

The analysis carried out in this work is based on observable quantities such as vibrational frequencies and electron density distributions. As noted above, the local mode frequencies calculated can be in principal measured[98,126,127] although experimental means for realizing routine measurements of local frequencies are still limited. Any set of measured frequencies, e.g. in the case of pnicogen-bonded dimers with C_{2h}-symmetry obtained by depolarized Raman scattering (in the case of C_i, C_2, C_s, or C_1 symmetry by terahertz spectroscopy), whether complete or incomplete, can be converted into local frequencies by the procedure developed by Cremer and co-workers.[125] Therefore, we predict that depolarized Raman spectroscopy and terahertz spectroscopy will play an important role to *measure* and characterize pnicogen bonding in complexes such as those presented in Figure 1.

Of course, except for **36** none of the dimers investigated in this work is stable at room temperature as is reflected by the calculated $\Delta G(298)$ values (Table 1), which are all positive. One has to decrease T to 100 K to observe **2**, **9**, **11**, **15**, **19**, and most of the heterodimers. By calculating $\Delta G(T)$ for different T, we have determined the value of T(obs) at which a given dimer should become observable. Considering the modern techniques of jet cooling, an observation should be possible for all dimers with a calculated $T \geq 100$ K.

So far, the analysis of pnicogen bonding has been carried out predominantly with calculated, nonobservable quantities, e.g., those that are calculated to rationalize the overall complex binding energy rather than the strength of the pnicogen bond. For example, results of an energy decomposition analysis[25,31,35,79] can be useful to understand ΔE values but cannot reveal the complex interplay between ΔE and k^a or relative BSOs as described in this work. In this respect, this work gives for the first time a quantitative measure of pnicogen bond strengths. We find that of 36 pnicogen bonded dimers only 10 have distinct covalent character (Figure 5) where all others are dominated by electrostatic E···E′ interactions where also dimers **4**, **22**, **24**, **31**, **32**, with very small negative H_b values have to be added to the latter category. We have obtained a similar predominance of electrostatic interactions when investigating H-bonding.[132] Finally, we have to note that we have used the term *pnicogen bonding* indiscriminately of the covalent or electrostatic nature or the strength of these interactions. Based on our results, it seems to be more appropriate in the future to speak of *covalent pnicogen bonding* and *electrostatic pnicogen interactions* depending on what term is appropriate.

Essential for pnicogen bonding is a charge transfer from D- to A-monomer in the sense of a through-space anomeric effect, which in the case of complexes such as **8** and **9** is better described as *through-space second-order hyperconjugation* or *through-space skewed π-conjugation* (Figure 2). In all these cases, charge transfer is enhanced by charge polarization effects where we show, in contrast to most previous investigations, that polarization effects, quantitatively assessed in this work by the local intermonomer bending force constants, can also be anticipated by a frontier orbital analysis of the monomers. This result is in line with the BLW analysis of Guan and Mo.[35] We also find that the electropositive (less electronegative) nature of E in the A-monomer combined with an electronegative ip substituent X guarantees an extension of the σ^*(EX) orbital into the intermonomer space (Figure 2). This effect is increased from N to P and to As because of increasing diffuseness of the valence orbitals. By this, E becomes sensitive to an increasing polarizing power of the D-monomer with decreasing atomic number of E (As, P, N; see **26**).

The variety of pnicogen interactions found in this work is significant, apart from the distinction into covalent and electrostatic interactions. It involves the mutual charge transfer via σ^*(EX) orbital in the homodimers leading to an increase of density closer to the E···E′ connection line (through-space anomeric effect) and the more π-related interactions with through-space second-order hyperconjugation or through-space skewed π-conjugation, which were previously described as *polarized systems*. A different type of pnicogen bonding is encountered in those cases that involve π^* orbitals (**29**, **34**, **35**, **36**). Though homodimers prefer an antiarrangement of ip EX bonds, heterodimers mostly adopt syn forms due to the attractive E, oop H interactions, which in the extreme can be supported by H-bonding. Dipole−dipole or in general multipole−multipole attraction between the D- and A-monomer can lead an increase in $|\Delta E|$. Pnicogen bonding is further characterized by the nature of the D and the A monomer in heterodimers, which can be identified by the approach taken in this investigation.

The strategy used in this work strongly differs from methods being based on the investigation of the electrostatic potential such as the *σ/π hole concept*.[29,50,80,81,143] Although these approaches may be useful for selected cases of pnicogen bonding, they lack the kinetic energy part required for the analysis of pnicogen bonding or the dimer stability. As pointed out by Ruedenberg[144] in his seminal work on the chemical bond, covalent interactions always imply a reduction of the kinetic energy and a balanced change in the potential energy, which cannot be assessed by considering just the electrostatic potential as was also pointed out by other authors.[40,56]

Similar limitations apply if the electron density is investigated to characterize pnicogen bonding. The existence of an electron density critical (3,−1) point does not verify the existence of a bond without using some additional criterion for covalent bonding as demonstrated by Cremer and Kraka.[115−117] The Laplacian of the electron density is for this purpose not suited because it contains according to the local virial theorem[114,117] the kinetic energy twice, which makes it difficult to use values of the Laplacian of $\rho(\mathbf{r})$ as bonding criteria. Recently, Eskandarii and Mahmoodabadi[82] made such an approach by using the Laplacian to reflect regions of excess kinetic or potential energy. This can only be done correctly by invoking electron density properties, which are directly related to the energy density rather than to its Laplacian.

The local mode analysis is based on the potential energy surface of a pnicogen bonded dimer and insofar it is not biased as electrostatic models are. Similarly, the energy density used in this work, if integrated over the total molecular space, leads to the dimer energy. These are the basic prerequisites for a rationalization of pnicogen bonding, which can also be applied for the characterization of chalcogen or halogen bonding.

■ ASSOCIATED CONTENT

Supporting Information

This contains calculated geometries, energies, NBO charges, bond distances and angles, and elecron and energy densities for all dimers, monomers, and reference molecules. A set of orbital pictures are given as well as a plot showing the intermonomer distance R as a function of the E···E′ stretching force constant k^a, and a plot showing the $|\Delta E|$ as a function of ρ_b. This material is available free of charge via the Internet at http://pubs.acs.org.

■ AUTHOR INFORMATION

Corresponding Author

*E. Kraka. E-mail: ekraka@smu.edu.

Notes

The authors declare no competing financial interest.

■ ACKNOWLEDGMENTS

This work was financially supported by the National Science Foundation, Grant CHE 1152357. We thank SMU for providing computational resources. Preliminary studies to this project by Paul Wiggins are acknowledged.

■ REFERENCES

(1) Hobza, P.; Müller-Dethlefs, K. *Noncovalent Interactions: Theory and Experiment*; Royal Society of Chemistry: Cambridge, U.K., 2010.

(2) Alkorta, I.; Blanco, F.; Deya, P. M.; Elguero, J.; Estarellas, C.; Frontera, A.; Quinonero, D. Cooperativity in Multiple Unusual Weak Bonds. *Theor. Chem. Acc.* **2014**, *126*, 1−14.

(3) Karshikof, A. *Non-covalent Interactions in Proteins*; World Scientific Publishing: Singapore, 2010.

(4) Sauvage, J. P.; Gaspard, P. *From Non-covalent Assemblies to Molecular Machines*; Wiley-VCH Verlag GmbH: Weinheim, 2010.

(5) Gilli, G.; Gilli, P. *The Nature of the Hydrogen Bond: Outline of a Comprehensive Hydrogen Bond Theory*; IUCr Monographs on Crystallography - 23; Oxford University Press: New York, 2009.

(6) Grabowski, S. J. *Hydrogen Bonding - New Insights*; Challenges and Advances in Computational Chemistry and Physics, Vol. 3; Springer: New York, 2006.

(7) Belkova, N. V.; Shubina, E. S.; Epstein, L. M. Diverse World of Unconventional Hydrogen Bonds. *Acc. Chem. Res.* **2005**, *38*, 624−631.

(8) Bakhmutov, V. I. *Dihydrogen Bond: Principles, Experiments, and Applications*; Wiley: New York, 2008.

(9) Wang, C.; Danovich, D.; Mo, Y.; Shaik, S. On the Nature of the Halogen Bond. *J. Chem. Theory Comput.* **2014**, *10*, 3726−3737.

(10) Scholfield, M. R.; Zanden, C. M. V.; Carter, M.; Ho, P. S. Halogen Bonding (XBonding): A Biological Perspective. *Protein Sci.* **2012**, *22*, 139−152.

(11) Wang, W.; Ji, B.; Zhang, Y. Chalcogen Bond: A Sister Noncovalent Bond to Halogen Bond. *J. Phys. Chem. A* **2009**, *113*, 8132−8135.

(12) Bleiholder, C.; Werz, D. B.; Köppel, H.; Gleiter, R. Theoretical Investigations on Chalcogen-Chalcogen Interactions: What Makes These Nonbonded Interactions Bonding? *J. Am. Chem. Soc.* **2006**, *128*, 2666−2674.

(13) Sánchez-Sanz, G.; Trujillo, C.; Alkorta, I.; Elguero, J. Intermolecular Weak Interactions in HTeXH Dimers (X = O, S, Se, Te): Hydrogen Bonds, Chalcogen-Chalcogen Contacts and Chiral Discrimination. *ChemPhysChem* **2012**, *13*, 496−503.

(14) Adhikari, U.; Scheiner, S. Effects of Charge and Substituent on the S···N Chalcogen Bond. *J. Phys. Chem. A* **2014**, *118*, 3183−3192.

(15) Hill, W. E.; Silva-Trivino, L. M. Preparation and Characterization of Di(tertiary phosphines) with Electronegative Substituents. 1. Symmetrical Derivatives. *Inorg. Chem.* **1978**, *17*, 2495−2498.

(16) Hill, W. E.; Silva-Trivino, L. M. Preparation and Characterization of Di(tertiary phosphines) with Electronegative Substituents. 2. Unsymmetrical Derivatives. *Inorg. Chem.* **1979**, *18*, 361−364.

(17) Drago, R. S.; Wong, N.; Ferris, D. C. The E, C, T Interpretation of Bond Dissociation Energies and Anion-Neutral Molecule Interactions. *J. Am. Chem. Soc.* **1991**, *113*, 1970−1977.

(18) Widhalm, M.; Kratky, C. Synthesis and X-ray Structure of Binaphthyl-Based Macrocyclic Diphosphanes and Their Ni(II) and Pd(II) Complexes. *Chem. Ber.* **1992**, *125*, 679−689.

(19) Carré, F.; Chuit, C.; Corriu, R. J. P.; Monforte, P.; Nayyar, N. K.; Reyè, C. Intramolecular Coordination at Phosphorus: Donor-Acceptor Interaction in Three- and Four-Coordinated Phosphorus Compounds. *J. Organomet. Chem.* **1995**, *449*, 147−154.

(20) Klinkhammer, K. W.; Pyykkö, P. Ab Initio Interpretation of the Closed-Shell Intermolecular E···E Attraction in Dipnicogen $(H_2E - EH_2)_2$ and Dichalcogen $(HE - EH)_2$ Hydride Model Dimers. *Inorg. Chem.* **1995**, *34*, 4134−4138.

(21) Kilian, P.; Slawin, A. M. Z.; Woollins, J. D. Naphthalene-1,8-diyl Bis(halogenophosphanes): Novel Syntheses and Structures of Useful Synthetic Building Blocks. *Chem.—Eur. J.* **2003**, *9*, 215−222.

(22) Sundberg, M.; Uggla, R.; Vinas, C.; Teixidor, F.; Paavola, S.; Kivekas, R. Nature of Intramolecular Interactions in Hypercoordinate C-Substituted 1,2-Dicarba-closododecaboranes with Short P···P Distances. *Inorg. Chem. Commun.* **2007**, *10*, 713−716.

(23) Tschirschwitz, S.; Lönnecke, P.; Hey-Hawkins, E. Amino-alkylferrocenyldichlorophosphanes: Facile Synthesis of Versatile Chiral Starting Materials. *Dalton Trans.* **2007**, 1377−1382.

(24) Ganesamoorthy, C.; Balakrishna, M. S.; Mague, J. T.; Tuononen, H. M. New Tetraphosphane Ligands $(X_2P)_2NC_6H_4N(PX_2)_2$ (X = Cl, F, OMe, OC_6H_4OMe-*o*): Synthesis, Derivatization, Group 10 and 11 Metal Complexes and Catalytic Investigations. DFT Calculations on Intermolecular P···P Interactions in Halo-Phosphines. *Inorg. Chem.* **2008**, *47*, 7035−7047.

(25) Moilanen, J.; Ganesamoorthy, C.; Balakrishna, M. S.; Tuononen, H. M. Weak Interactions between Trivalent Pnictogen Centers: Computational Analysis of Bonding in Dimers $X_3E\cdots EX_3$ (E = Pnictogen, X = Halogen). *Inorg. Chem.* **2009**, *48*, 6740−6747.

(26) Zahn, S.; Frank, R.; Hey-Hawkins, E.; Kirchner, B. Pnicogen Bonds: A New Molecular Linker? *Chem.—Eur. J.* **2011**, *17*, 6034−6038.

(27) Bauer, S.; Tschirschwitz, S.; Lönnecke, P.; Frank, R.; Kirchner, B.; Clarke, M. L.; Hey-Hawkins, E. Enantiomerically Pure Bis(phosphanyl)carbaborane(12) Compounds. *Eur. J. Inorg. Chem.* **2009**, 2776−2788.

(28) Del Bene, J.; Alkorta, I.; Elguero, J. σ-σ and σ-π Pnicogen Bonds in Complexes H_2XP:PCX, for X = F, Cl, OH, NC, CN, CCH, CH_3, and H. *Theor. Chem. Acc.* **2014**, *133*, 1464−1473.

(29) Del Bene, J. E.; Alkorta, I.; Elguero, J. Properties of Complexes $H_2C(X)P$: PXH_2, for X = F, Cl, OH, CN, NC, CCH, H, CH_3, and BH_2: P···P Pnicogen Bonding at σ-Holes and π-Holes. *J. Phys. Chem. A* **2013**, *117*, 11592−11604.

(30) Alkorta, I.; Elguero, J. Pnicogen-Bonded Cyclic Trimers $(PH_2X)_3$ with X = F, Cl, OH, NC, CN, CH_3, H, and BH_2. *J. Phys. Chem. A* **2013**, *117*, 4981−4987.

(31) Del Bene, J.; Alkorta, I.; Sánchez-Sanz, G.; Elguero, J. Structures, Binding Energies, and Spin-Spin Coupling Constants of Geometric Isomers of Pnicogen Homodimers $(PHFX)_2$, X = F, Cl, CN, CH_3, NC. *J. Phys. Chem. A* **2012**, *116*, 3056−3060.

(32) Del Bene, J.; Sánchez-Sanz, G.; Alcorta, I.; Elguero, J. Homo- and Heterochiral Dimers $(PHFX)_2$, X = Cl, CN, CH_3, NC: To What Extent Do They Differ? *J. Chem. Phys. Lett.* **2012**, *538*, 14−18.

(33) Sanz, D.; Claramunt, R. M.; Mathey, F.; Alkorta, I.; Sánchez-Sanz, G.; Elguero, J. Intermolecular Spin-Spin Coupling Constants between ^{31}P Atoms. *C. R. Chimie* **2013**, *16*, 937−944.
(34) Del Bene, J.; Alcorta, I.; Sánchez-Sanz, G.; Elguero, J. $^{31}P-^{31}P$ Spin-Spin Coupling Constants for Pnicogen Homodimers. *Chem. Phys. Lett.* **2011**, *512*, 184−187.
(35) Guan, L.; Mo, Y. Electron Transfer in Pnicogen Bonds. *J. Phys. Chem. A* **2014**, *118*, 8911−8921.
(36) Del Bene, J. E.; Alkorta, I.; Sánchez-Sanz, G.; Elguero, J. Phosphorus as a Simultaneous Electron-Pair Acceptor in Intermolecular P· · ·N Pnicogen Bonds and Electron- Pair Donor to Lewis Acids. *J. Phys. Chem. A* **2013**, *117*, 3133−3141.
(37) Alkorta, I.; Sánchez-Sanz, G.; Elguero, J. Pnicogen Bonds between X═PH_3 (X = O, S, NH, CH_2) and Phosphorus and Nitrogen Bases. *J. Phys. Chem. A* **2014**, *118*, 1527−1537.
(38) Alkorta, I.; Elguero, J. Pnicogen Bonded Complexes of PO_2X (X = F, Cl) with Nitrogen Bases. *J. Phys. Chem. A* **2013**, *117*, 10497−10503.
(39) Del Bene, J.; Alkorta, I.; Sánchez-Sanz, G.; Elguero, J. Structures, Energies, Bonding, and NMR Properties of Pnicogen Complexes of H_2XP-NXH_2 (X = H, CH_3, NH_2, OH, F, Cl). *J. Phys. Chem. A* **2011**, *115*, 13724−13731.
(40) Scheiner, S. A New Noncovalent Force: Comparison of P···N Interaction with Hydrogen and Halogen Bonds. *J. Chem. Phys.* **2011**, *134*, 094315−1−4.
(41) Scheiner, S. Effects of Substituents upon the P···N Noncovalent Interaction: The Limits of Its Strength. *J. Phys. Chem. A* **2011**, *115*, 11202−11209.
(42) Adhikari, U.; Scheiner, S. Effects of Carbon Chain Substituents on the P···N Noncovalent Bond. *Chem. Phys. Lett.* **2012**, *536*, 30−33.
(43) Scheiner, S. Can Two Trivalent N Atoms Engage in a Direct N···N Noncovalent Interaction? *Chem. Phys. Lett.* **2011**, *514*, 32−35.
(44) An, X.; Li, R.; Li, Q.; Liu, X.; Li, W.; Cheng, J. Substitution, Cooperative, and Solvent Effects on π Pnicogen Bonds in the FH_2P and FH_2As Complexes. *J. Mol. Model* **2012**, *18*, 4325−4332.
(45) Politzer, P.; Murray, S. J.; Concha, M. σ-Hole Bonding between Like Atoms, A Fallacy of Atomic Charges. *J. Mol. Model.* **2008**, *14*, 659−665.
(46) Li, Q.; Zhuo, H.; Yang, X.; Cheng, J.; Li, W.; Loffredo, R. E. Cooperative and Diminutive Effects of Pnicogen Bonds and Cation-π Interactions. *ChemPhysChem* **2014**, *15*, 500−506.
(47) Del Bene, J.; Alkorta, I.; Elguero, J. Pnicogen-Bonded Anionic Complexes. *J. Phys. Chem. A* **2014**, *118*, 3386−3392.
(48) Chen, Y.; Yao, L.; Lin, X. Theoretical Study of $(FH_2X)_n$·Y (X = P and As, n = 1−4, Y = F, Cl, Br, I, NO_3 and SO_2^4): The Possibility of Anion Recognition Based on Pnicogen Bonding. *Protein Sci.* **2014**, *22*, 44−50.
(49) Ma, F.; Li, A. A Computational Study of Pnicogen-Hydride Interaction in Complexes XH_2P···HBeY. *Comput. Theor. Chem.* **2014**, *1045*, 78−85.
(50) Del Bene, J. E.; Alkorta, I.; Elguero, J. Characterizing Complexes with Pnicogen Bonds Involving sp^2 Hybridized Phosphorus Atoms: $(H_2C{=}PX)_2$ with X = F, Cl, OH, CN, NC, CCH, H, CH_3, and BH_2. *J. Phys. Chem. A* **2013**, *117*, 6893−6903.
(51) Sánchez-Sanz, G.; Alkorta, I.; Trujillo, C.; Elguero, J. Intramolecular Pnicogen Interactions in PHF-$(CH_2)_n$-PHF (n=2−6) Systems. *ChemPhysChem* **2013**, *14*, 1656−1665.
(52) Sánchez-Sanz, G.; Trujillo, C.; Solimannejad, M.; Alkorta, I.; Elguero, J. Orthogonal Interactions between Nitryl Derivatives and Electron Donors: Pnictogen Bonds. *Phys. Chem. Chem. Phys.* **2013**, *15*, 14310−14318.
(53) Bauzá, A.; Ramis, R.; Frontera, A. A Combined Theoretical and Cambridge Structural Database Study of π-Hole Pnicogen Bonding Complexes between Electron Rich Molecules and Both Nitro Compounds and Inorganic Bromides (YO_2Br, Y = N, P, and As). *J. Phys. Chem. A* **2014**, *118*, 2827−2834.
(54) Alkorta, I.; Elguero, J.; Solimannejad, M. Single Electron Pnicogen Bonded Complexes. *J. Phys. Chem. A* **2014**, *118*, 947−953.
(55) Bauzá, A.; Quinonero, D.; Deyá, P. M.; Frontera, A. Pnicogen-π Complexes: Theoretical Study and Biological Implications. *Phys. Chem. Chem. Phys.* **2012**, *14*, 14061−14066.
(56) Scheiner, S. The Pnicogen Bond: Its Relation to Hydrogen, Halogen, and Other Noncovalent Bonds. *Acc. Chem. Res.* **2013**, *46*, 280−288.
(57) Scheiner, S. Detailed Comparison of the Pnicogen Bond with Chalcogen, Halogen, and Hydrogen Bonds. *Int. J. Quantum Chem.* **2013**, *113*, 1609−1620.
(58) Scheiner, S. Sensitivity of Noncovalent Bonds to Intermolecular Separation: Hydrogen, Halogen, Chalcogen, and Pnicogen Bonds. *CrystEngComm* **2013**, *15*, 3119−3124.
(59) Bauzá, A.; Quinonero, D.; Deyá, P. M.; Frontera, A. Halogen Bonding versus Chalcogen and Pnicogen Bonding: Combined Cambridge Structural Database and Theoretical Study. *Cryst. Eng. Comm* **2013**, *15*, 3137−3144.
(60) George, J.; Deringer, V. L.; Dronskowski, R. Cooperativity of Halogen, Chalcogen, and Pnictogen Bonds in Infinite Molecular Chains by Electronic Structure Theory. *J. Phys. Chem. A* **2014**, *118*, 3193−3200.
(61) Li, Q.; Zhu, H.; Zhuo, H.; Yang, X.; Li, W.; Cheng, J. Complexes between Hypohalous Acids and Phospine Derivatives. Pnicogen Bond versus Halogen Bond versus Hydrogen Bond. *Spectrochim. Acta, Part A* **2014**, *132*, 271−277.
(62) Bauzá, A.; Alkorta, I.; Frontera, A.; Elguero, J. On the Reliability of Pure and Hybrid DFT Methods for the Evaluation of Halogen, Chalcogen, and Pnicogen Bonds Involving Anionic and Neutral Electron Donors. *J. Chem. Theory Comput.* **2013**, *9*, 5201−5210.
(63) Alkorta, I.; Sánchez-Sanz, G.; Elguero, J.; Del Bene, J. E. Exploring $(NH_2F)_2$, H_2FP:NFH_2, and $(PH_2F)_2$ Potential Surfaces: Hydrogen Bonds or Pnicogen Bonds? *J. Phys. Chem. A* **2013**, *117*, 183−191.
(64) Liu, X.; Cheng, J.; Li, Q.; Li, W. Competition of Hydrogen, Halogen, and Pnicogen Bonds in the Complexes of HArF with XH_2P (X = F, Cl, and Br). *Spectrochim. Acta, Part A* **2013**, *101*, 172−177.
(65) Li, Q.; Li, R.; Liu, X.; Li, W.; Cheng, J. Concerted Interaction between Pnicogen and Halogen Bonds in XCl-FH_2P-NH_3 (X = F, OH, CN, NC, FCC). *ChemPhysChem* **2012**, *13*, 1205−1212.
(66) Li, Q.; Li, R.; Liu, X.; Li, W.; Cheng, J. Pnicogen Hydride Interaction between FH_2X (X = P and As) and HM (M = ZnH, BeH, MgH, Li, and Na). *J. Phys. Chem. A* **2012**, *116*, 2547−2553.
(67) Del Bene, J.; Alkorta, I.; Sánchez-Sanz, G.; Elguero, J. Interplay of F-H···F Hydrogen Bonds and P···N Pnicogen Bonds. *J. Phys. Chem. A* **2012**, *116*, 9205−9213.
(68) Alkorta, I.; Sánchez-Sanz, G.; Elguero, J.; Del Bene, J. Influence of Hydrogen Bonds on the P··· P Pnicogen Bond. *J. Chem. Theory Comput.* **2012**, *8*, 2320−2327.
(69) Adhikari, U.; Scheiner, S. Sensitivity of Pnicogen, Chalcogen, Halogen and H-Bonds to Angular Distortions. *Chem. Phys. Lett.* **2012**, *532*, 31−35.
(70) Adhikari, U.; Scheiner, S. Comparison of P···D (D = P, N) with Other Noncovalent Bonds in Molecular Aggregates. *J. Chem. Phys.* **2011**, *135*, 184306−1−9.
(71) Adhikari, U.; Scheiner, S. Substituent Effects on Cl···N, S···N, and P···N Noncovalent Bonds. *J. Phys. Chem. A* **2012**, *116*, 3487−3497.
(72) von Hopffgarten, M.; Frenking, G. Energy Decomposition Analysis. *Wiley Interdiscip. Rev.: Comput. Mol. Sci.* **2012**, *2*, 43−62.
(73) Sherrill, C. D. Energy Component Analysis of π Interactions. *Acc. Chem. Res.* **2013**, *46*, 1020−1028.
(74) Jeziorski, B.; Moszynski, R.; Szalewicz, K. Perturbation Theory Approach to Intermolecular Potential Energy Surfaces of van der Waals Complexes. *Chem. Rev.* **1994**, *94*, 1887−1930.
(75) Szalewicz, K. Energy Component Analysis of π Interactions. *Wiley Interdiscip. Rev.: Comput. Mol. Sci.* **2012**, *2*, 254−272.
(76) Su, P.; Jiang, Z.; Chen, Z.; Wu, W. Energy Decomposition Scheme Based on the Generalized Kohn-Sham Scheme. *J. Phys. Chem. A* **2014**, *118*, 2531−2542.

(77) Corminboeuf, C. Minimizing Density Functional Failures for Non-Covalent Interactions Beyond van der Waals Complexes. *Acc. Chem. Res.* **2014**, DOI: 10.1021/ar400303a.
(78) Steinmann, S. N.; Piemontesi, C.; Delachat, A.; Corminboeuf, C. Why Are the Interaction Energies of Charge-Transfer Complexes Challenging for DFT? *J. Chem. Theory Comput.* **2012**, *8*, 1629−1640.
(79) Mo, Y.; Bao, P.; Gao, J. Energy Decomposition Analysis Based on a Block-Localized Wave Functions and Multistage Density Functional Theory. *Phys. Chem. Chem. Phys.* **2011**, *13*, 6760−6775.
(80) Murray, J. S.; Macaveiu, L.; Politzer, P. Factors Affecting the Strengths of σ-Hole Electrostatic Potentials. *J. Comput. Sci.* **2014**, *5*, 590−596.
(81) Murray, J. S.; Lane, P.; Politzer, P. A Predicted New Type of Directional Noncovalent Interaction. *Int. J. Quantum Chem.* **2007**, *107*, 2286−2292.
(82) Eskandari, K.; Mahmoodabadi, N. Pnicogen Bonds: A Theoretical Study Based on the Laplacian of Electron Density. *J. Phys. Chem. A* **2013**, *117*, 13018−13024.
(83) Sánchez-Sanz, G.; Trujillo, C.; Alkorta, I.; Elguero, J. Electron Density Shift Description of Non-bonding Intramolecular Interactions. *Comp. Theor. Chem.* **2012**, *991*, 124−133.
(84) Steiner, T. The Hydrogen Bond in the Solid State. *Angew. Chem., Int. Ed.* **2002**, *41*, 48−76.
(85) Diken, E. G.; Headrick, J. M.; Roscioli, J. R.; Bopp, J. C.; Johnson, M. A.; McCoy, A. Fundamental Excitations of the Shared Proton in the $H_3O_2^-$ and $H_5O_2^+$ Complexes. *J. Phys. Chem. A* **2005**, *109*, 1487−1490.
(86) Diken, E. G.; Headrick, J. M.; Roscioli, J. R.; Bopp, J. C.; McCoy, A. B.; Huang, X.; Carter, S.; Bowman, J. M. Argon Predissociation Spectroscopy of the $OH^-{\cdot}H_2O$ and $Cl^-{\cdot}H_2O$ Complexes in the 1000−1900 cm^{-1} Region: Intramolecular Bending Transitions and the Search for the Shared-Proton Fundamental in the Hydroxide Monohydrate. *J. Phys. Chem. A* **2005**, *109*, 571−575.
(87) Grabowski, S. J. Red- and Blue-Shifted Hydrogen Bonds: The Bent Rule from Quantum Theory of Atoms in Molecules Perspective. *J. Phys. Chem. A* **2011**, *115*, 12789−12799.
(88) Heisler, I. A.; Meech, S. R. Low-Frequency Modes of Aqueous Alkali Halide Solutions: Glimpsing the Hydrogen Bonding Vibration. *Science* **2010**, *327*, 857−860.
(89) Elsaesser, T. Two-Dimensional Infrared Spectroscopy of Intermolecular Hydrogen Bonds in the Condensed Phase. *Acc. Chem. Res.* **2009**, *42*, 1220−1228.
(90) Freindorf, M.; Kraka, E.; Cremer, D. A Comprehensive Analysis of Hydrogen Bond Interactions Based on Local Vibrational Modes. *Int. J. Quantum Chem.* **2012**, *112*, 3174−3187.
(91) Kalescky, R.; Zou, W.; Kraka, E.; Cremer, D. Local Vibrational Modes of the Water Dimer - Comparison of Theory and Experiment. *Chem. Phys. Lett.* **2012**, *554*, 243−247.
(92) McIntosh, A. I.; Yang, B.; Goldup, S. M.; Watkinson, M.; Donnan, R. S. Terahertz Spectroscopy: A Powerful New Tool for the Chemical Sciences? *Chem. Soc. Rev.* **2012**, *41*, 2072−2082.
(93) Mantsch, H. H.; Naumann, D. Terahertz Spectroscopy: The Renaissance of Far Infrared Spectroscopy. *J. Mol. Struct.* **2010**, *964*, 1−4.
(94) Parrott, E. P. J.; Sun, Y.; Pickwell-MacPherson, E. Terahertz Spectroscopy: Its Future Role in Medical Diagnoses. *J. Mol. Struct.* **2011**, *1006*, 66−76.
(95) Konkoli, Z.; Cremer, D. A New Way of Analyzing Vibrational Spectra. I. Derivation of Adiabatic Internal Modes. *Int. J. Quantum Chem.* **1998**, *67*, 1−9.
(96) Konkoli, Z.; Cremer, D. A New Way of Analyzing Vibrational Spectra. III. Characterization of Normal Vibrational Modes in Terms of Internal Vibrational Modes. *Int. J. Quantum Chem.* **1998**, *67*, 29−40.
(97) Zou, W.; Kalescky, R.; Kraka, E.; Cremer, D. Relating Normal Vibrational Modes to Local Vibrational Modes with the Help of an Adiabatic Connection Scheme. *J. Chem. Phys.* **2012**, *137*, 084114-1−11.
(98) Zou, W.; Cremer, D. Properties of Local Vibrational Modes: The Infrared Intensity. *Theor. Chem. Acc.* **2014**, *133*, 1451−1−15.
(99) Chai, J. D.; Head-Gordon, M. Long-range Corrected Hybrid Density Functionals with Damped Atom-Atom Dispersion Corrections. *Phys. Chem. Chem. Phys.* **2008**, *10*, 6615−6620.
(100) Chai, J. D.; Head-Gordon, M. Systematic Optimization of Long-Range Corrected Hybrid Density Functionals. *J. Chem. Phys.* **2008**, *128*, 084106−15.
(101) Thanthiriwatte, K. S.; Hohenstein, E. G.; Burns, L. A.; Sherrill, C. D. Assessment of the Performance of DFT and DFT-D Methods for Describing Distance Dependence of Hydrogen-Bonded Interactions. *J. Chem. Theory Comput.* **2011**, *7*, 88−96.
(102) Kozuch, S.; Martin, J. M. L. Halogen Bonds: Benchmarks and Theoretical Analysis. *J. Chem. Theory Comput.* **2013**, *9*, 1918−1931.
(103) Scheiner, S. Extrapolation to the Complete Basis Set Limit for Binding Energies of Noncovalent Interactions. *Comput. Theor. Chem.* **2012**, *998*, 9−13.
(104) Woon, D. E.; Dunning, T. H., Jr. Gaussian Basis Sets for Use in Correlated Molecular Calculations. IV. Calculation of Static Electrical Response Properties. *J. Chem. Phys.* **1994**, *100*, 2975−2988.
(105) Woon, D. E.; Dunning, T. H., Jr. Gaussian Basis Sets for Use in Correlated Molecular Calculations. III. The Atoms Aluminum through Argon. *J. Chem. Phys.* **1993**, *98*, 1358−1371.
(106) Wilson, A. K.; Woon, D. E.; Peterson, K. A.; Dunning, T. H., Jr. Gaussian Basis Sets for Use in Correlated Molecular Calculations. IX. The Atoms Gallium through Krypton. *J. Chem. Phys.* **1999**, *110*, 7667−7676.
(107) Metz, B.; Stoll, H.; Dolg, M. Small-core Multiconfiguration-Dirac-Hartree-Fockadjusted Pseudopotentials for Post-d Main Group Elements: Application to PbH and PbO. *J. Chem. Phys.* **2000**, *113*, 2563−2469.
(108) Peterson, K. A.; Figgen, D.; Goll, E.; Stoll, H.; Dolg, M. Systematically Convergent Basis Sets with Relativistic Pseudopotentials. II. Small-Core Pseudopotentials and Correlation Consistent Basis Sets for the Post-d Group 16−18 Elements. *J. Phys. Chem. A* **2003**, *119*, 11113−11124.
(109) Peterson, K. A.; Shepler, B. C.; Figgen, D.; Stoll, H. On the Spectroscopic and Thermochemical Properties of ClO, BrO, IO, and Their Anions. *J. Phys. Chem. A* **2006**, *110*, 13877−13883.
(110) Raghavachari, K.; Trucks, G. W.; Pople, J. A.; Head-Gordon, M. A Fifth-order Perturbation Comparison of Electron Correlation Theories. *Chem. Phys. Lett.* **1989**, *157*, 479−483.
(111) Boys, S. F.; Bernardi, F. The Calculation of Small Molecular Interactions by the Differences of Separate Total Energies. Some Procedures with Reduced Errors. *Mol. Phys.* **1970**, *19*, 553−566.
(112) Reed, A. E.; Curtiss, L. A.; Weinhold, F. Intermolecular Interactions From a Natural Bond Orbital, Donor-Acceptor Viewpoint. *Chem. Rev.* **1988**, *88*, 899−926.
(113) Weinhold, F.; Landis, C. R. *Valency and Bonding: A Natural Bond Orbital Donor- Acceptor Perspective*; Cambridge University Press: Cambridge, U.K., 2003.
(114) Bader, R. F. W. *Atoms in Molecules: A Quantum Theory*; Oxford University Press: Oxford, U.K., 1994.
(115) Cremer, D.; Kraka, E. A Description of the Chemical Bond in Terms of Local Properties of Electron Density and Energy. *Croat. Chem. Acta* **1984**, *57*, 1259−1281.
(116) Cremer, D.; Kraka, E. Chemical Bonds without Bonding Electron Density - Does the Difference Electron Density Analysis Suffice for a Description of the Chemical Bond? *Agnew. Chem. Int. Ed. Engl.* **1984**, *23*, 627−628.
(117) Kraka, E.; Cremer, D. In Theoretical Models of Chemical Bonding. *The Concept of the Chemical Bond*; Maksic, Z. B., Ed.; Springer Verlag, Heidelberg, 1990; Vol 2, p 453.
(118) Hariharan, P. C.; Pople, J. A. The Influence of Polarization Functions on Molecular Orbital Hydrogenation Energies. *Theor. Chim. Acta* **1973**, *28*, 213−222.
(119) Krishnan, R.; Binkley, J. S.; Seeger, R.; Pople, J. A. Self-Consistent Molecular Orbital Methods. XX. A Basis Set for Correlated Wave Functions. *J. Chem. Phys.* **1980**, *72*, 650−654.

(120) Kraka, E.; Zou, W.; Filatov, M.; Grafenstein, J.; Izotov, D.; Gauss, J.; He, Y.; Wu, A.; Konkoli, Z.; Cremer, D.; et al. *COLOGNE2014*, 2014; http://www.smu.edu/catco.
(121) Stanton, J. F.; Gauss, J.; Harding, M. E.; Szalay, P. G. *CFOUR*, 2010; http://www.cfour.de.
(122) Harding, M. E.; Mezroth, T.; Gauss, J.; Auer, A. A. Parallel Calculation of CCSD and CCSD(T) Analytic First and Second Derivatives. *J. Chem. Theory Comput.* **2008**, *4*, 64.
(123) Werner, H. J.; Knowles, P. J.; Knizia, G.; Manby, F. R.; Schütz, M.; Celani, P.; Korona, T.; Lindh, R.; Mitrushenkov, A.; Rauhut, G.; et al. *MOLPRO*, Version 2010.1, A Package of Ab Initio Programs. 2010; http://www.molpro.net.
(124) Frisch, M. J.; Trucks, G. W.; Schlegel, H. B.; Scuseria, G. E.; Robb, M. A.; Cheeseman, J. R.; Scalmani, G.; Barone, V.; Mennucci, B.; Petersson, G. A.; et al. *Gaussian 09*, Revision A. 1; Gaussian Inc.: Wallingford, CT, 2010.
(125) Cremer, D.; Larsson, J. A.; Kraka, E. In *Theoretical Organic Chemistry*; Parkanyi, C., Ed.; Theoretical and Computational Chemistry, Vol *5*; Elsevier: Amsterdam, 1998; pp 259−327.
(126) Kraka, E.; Larsson, J. A.; Cremer, D. In *Computational Spectroscopy: Methods, Experiments and Applications*; Grunenberg, J., Ed.; Wiley: New York, 2010; pp 105−149.
(127) Cremer, D.; Kraka, E. From Molecular Vibrations to Bonding, Chemical Reactions, and Reaction Mechanism. *Curr. Org. Chem.* **2010**, *14*, 1524−1560.
(128) McKean, D. C. Individual CH Bond Strengths in Simple Organic Compounds: Effects of Conformation and Substitution. *Chem. Soc. Rev.* **1978**, *7*, 399−422.
(129) Henry, B. R. The Local Mode Model and Overtone Spectra: A Probe of Molecular Structure and Conformation. *Acc. Chem. Res.* **1987**, *20*, 429−435.
(130) Wilson, E. B.; Decius, J. C.; Cross, P. C. Molecular Vibrations. *The Theory of Infrared and Raman Vibrational Spectra*; McGraw-Hill: New York, 1955.
(131) Zou, W.; Kalescky, R.; Kraka, E.; Cremer, D. Relating Normal Vibrational Modes to Local Vibrational Modes Benzene and Naphthalene. *J. Mol. Model.* **2012**, 1−13.
(132) Freindorf, M.; Kraka, E.; Cremer, D. A Comprehensive Analysis of Hydrogen Bond Interactions Based on Local Vibrational Modes. *Int. J. Quantum Chem.* **2012**, *112*, 3174−3187.
(133) Kraka, E.; Cremer, D. Characterization of CF Bonds with Multiple-bond Character: Bond Lengths, Stretching Force Constants, and Bond Dissociation Energies. *ChemPhysChem* **2009**, *10*, 686−698.
(134) Kalescky, R.; Zou, W.; Kraka, E.; Cremer, D. Quantitative Assessment of the Multiplicity of Carbon-Halogen Bonds: Carbenium and Halonium Ions with F, Cl, Br, I. *J. Phys. Chem. A* **2014**, *118*, 1948−1963.
(135) Kalescky, R.; Kraka, E.; Cremer, D. Identification of the Strongest Bonds in Chemistry. *J. Phys. Chem. A* **2013**, *117*, 8981−8995.
(136) Badger, R. M. A Relation between Internuclear Distances and Bond Force Constants. *J. Chem. Phys.* **1934**, *2*, 128−131.
(137) Cremer, D. In *The Chemistry of Functional Groups, Peroxides*; Patai, S., Ed.; Wiley: New York, 1983; pp 1−84.
(138) Thatcher, G. R. J. *The Anomeric Effect and Associated Stereoelectronic Effects*; American Chemical Society; Washington, DC, 1993.
(139) Albright, T. A.; Burdett, J. K.; Whangbo, M.-H. *Orbital Interactions in Chemistry*; Wiley: New York, 2013.
(140) Murray, J. S.; Lane, P.; Clark, T.; Riley, K. E.; Politzer, P. σ-Holes, π-Holes and Electrostatically-Driven Interactions. *J. Mol. Model.* **2012**, *18*, 541−548.
(141) Lide, D. R. *CRC Handbook of Chemistry and Physics on CD-ROM*; CRC Press LLC: Boca Raton, FL, 2000.
(142) Scheiner, S. Effects of Multiple Substitution upon the N···N Noncovalent Interaction. *Chem. Phys.* **2011**, *387*, 79−84.
(143) Clark, T.; Henneman, M.; Murray, J. S.; Politzer, P. Halogen Bonding: The σ-Hole. *J. Mol. Model.* **2007**, *13*, 291−296.
(144) Ruedenberg, K. The Physical Nature of the Chemical Bond. *Rev. Mod. Phys.* **1962**, *34*, 326−352.